



Minnesota
Department of
Transportation

RESEARCH SERVICES

Office of
Policy Analysis,
Research &
Innovation

Automated Vehicle Location, Data Recording, Friction Measurement and Applicator Control for Winter Road Maintenance

Rajesh Rajamani, Principal Investigator
Department of Mechanical Engineering
University of Minnesota

February 2010

Research Project
Final Report #2010-07

Your Destination... Our Priority



Technical Report Documentation Page

1. Report No. MN/RC 2010-07	2.	3. Recipients Accession No.	
4. Title and Subtitle Automated Vehicle Location, Data Recording, Friction Measurement and Applicator Control for Winter Road Maintenance		5. Report Date February 2010	
		6.	
7. Author(s) Gurkan Erdogan, Lee Alexander and Rajesh Rajamani		8. Performing Organization Report No.	
9. Performing Organization Name and Address Department of Mechanical Engineering University of Minnesota 111 Church Street S.E. Minneapolis, MN 55455		10. Project/Task/Work Unit No.	
		11. Contract (C) or Grant (G) No. (c) 89261 (wo) 58	
12. Sponsoring Organization Name and Address Minnesota Department of Transportation Research Services Section 395 John Ireland Boulevard, MS 330 St. Paul, MN 55155-1899		13. Type of Report and Period Covered Final Report	
		14. Sponsoring Agency Code	
15. Supplementary Notes http://www.lrrb.org/pdf/201007.pdf			
16. Abstract (Limit: 250 words) The first part of this project conducted a detailed evaluation of the ability of a new friction measurement system to provide an accurate measure of road conditions. A system that records friction coefficient as a function of road location was developed using the same vehicle location measurement system as the current MDSS project. Studies conducted show that the friction measurement system provides a significantly more reliable measure of road surface conditions than does visual inspection. The second part of this project focused on a detailed evaluation of the performance of a closed-loop system that utilizes friction measurement for automatic applicator control. Experimental studies have shown that a friction measurement based zero velocity sander can adequately apply salt/chemicals to all slippery spots on a road at speeds up to 25 mph. The final part of this project focused on enhancement of the developed automatic applicator control system with utilization of real-time data from a geographical information system that provides information on upcoming geometric road alignment and known problematic segments of roadway. The developed friction measurement, data recording and applicator control system is compact, modular and can be used on both snowplows and pick-up trucks.			
17. Document Analysis/Descriptors Coefficient of friction, Tires, Snowplows, Snowplow applicator control, Snow and ice control, Winter road maintenance		18. Availability Statement No restrictions. Document available from: National Technical Information Services, Springfield, Virginia 22161	
19. Security Class (this report) Unclassified	20. Security Class (this page) Unclassified	21. No. of Pages 61	22. Price

Automated Vehicle Location, Data Recording, Friction Measurement and Applicator Control for Winter Road Maintenance

Final Report

Prepared by:

Gurkan Erdogan
Lee Alexander
Rajesh Rajamani

Department of Mechanical Engineering
University of Minnesota

February 2010

Published by:

Minnesota Department of Transportation
Research Services Section
395 John Ireland Boulevard, MS 330
St. Paul, Minnesota 55155-1899

This report represents the results of research conducted by the authors and does not necessarily represent the views or policies of the Minnesota Department of Transportation or the University of Minnesota. This report does not contain a standard or specified technique.

The authors, the Minnesota Department of Transportation and the University of Minnesota do not endorse products or manufacturers. Any trade or manufacturers' names that may appear herein do so solely because they are considered essential to this report.

Acknowledgments

The research team would like to thank Jack Herndon and the staff at MnROAD for their help in facilitating the experimental work carried out in this project. We are also grateful to Cliff Gergen and the staff at the Mn/DOT truck station at Lakeville for facilitating the use of the zero velocity sander. Finally, we would like to thank Gabe Guevara and all other members of the Technical Advisory Panel for their feedback and guidance during this project.

Table of Contents

CHAPTER 1. INTRODUCTION	1
1.1 Winter Road Maintenance	1
1.2 Review of Friction Measurement Systems	2
a) Vehicle Based Systems	2
b) Wheel Based Systems	3
c) Tire Based Systems	3
1.3 Project Contributions	3
CHAPTER 2. FRICTION MEASUREMENT SYSTEM AND ITS EVALUATION	5
2.1 Conventional Friction Estimation Method.....	5
2.2 Advantages of New Wheel Based System.....	5
2.3 New Wheel Based Friction Estimation System	6
2.4 Design Constraints	6
2.5 Friction Coefficient Measurement System	7
2.6 Technical Challenges	9
a) Influence of Vibrations	9
b) Influence of Vehicle Maneuvers	10
2.7 Correlation of Force and Acceleration Signals	11
2.8 Cross-Correlation Based Vibration Cancellation.....	12
2.9 Adaptive Feed-Forward Filter for Vibration Cancellation	14
2.10 Change Detection Algorithm	16
2.11 Experimental Results	17
2.12 Cancellation of Vehicle Maneuvers.....	22
a) Effects of Acceleration and Deceleration	22
b) Cancellation of Lateral Vehicle Maneuvers	22
2.13 Biased Quadratic Mean Filter	25
CHAPTER 3. CLOSED LOOP APPLICATOR CONTROL	28
3.1 Friction Mapping with Automatic Vehicle Location.....	28
3.2 Black Ice and Wet Surface Differentiation	32
3.3 Measurement of Snowplow Applicator Delay.....	35
3.4 Measurement of Friction Measurement System Delay.....	39
3.5 Analysis of Total Delay and Closed-Loop Performance	41
3.6 GIS Based Applicator Control	42
3.7 Description of Hardware.....	45
CHAPTER 4. CONCLUSIONS.....	49
REFERENCES.....	51

List of Tables

Table 2.1 Truck Speeds vs. Available Times for Data Processing and Applicator Activation 7

List of Figures

Figure 2.1 Photograph of the Norse Meter	5
Figure 2.2 Winter Road Maintenance System	6
Figure 2.3 Plan View Schematic of the Wheel Based System	7
Figure 2.4 Photograph of the Wheel Based System	8
Figure 2.5 Frequency Spectrum of a Typical Force Signal	9
Figure 2.6 Typical Load-Cell Signals Before and After Low Pass Filtering ($f_c=5\text{Hz}$)	10
Figure 2.7 Typical Load-Cell Signals Before and After Low Pass Filtering ($f_c=0.5\text{ Hz}$)	10
Figure 2.8 Accelerometer and Load Cell Locations	11
Figure 2.9 Low Pass Filtered Load-Cell and Acceleration Signals ($f_c=10\text{Hz}$)	12
Figure 2.10 Time Delay between the Load-Cell and Accelerometer Signals.....	12
Figure 2.11 Block Diagram of Proposed Estimation Algorithm	14
Figure 2.12 Skid-Pad Test Environments	17
Figure 2.13 Tire-Road Friction Coefficient Estimation at 20 mph.....	18
Figure 2.14 Tire-Road Friction Coefficient Estimation at 30 mph.....	19
Figure 2.15 Tire-Road Friction Coefficient Estimation at 35 mph.....	19
Figure 2.16 Tire-Road Friction Coefficient Estimation at 40 mph.....	20
Figure 2.17 Adaptive Feedforward vs. Traditional LPF at 30 mph.....	20
Figure 2.18 Adaptive Feedforward vs. Traditional LPF at 35 mph.....	21
Figure 2.19 Effect of Acceleration and Deceleration of the Snowplow	22
Figure 2.20 Accelerometer and Load Cell Data during Lateral Steering Maneuver	23
Figure 2.21 Accelerometer and Load Cell Data after Low Pass Filtering.....	24
Figure 2.22 Friction Coefficient after Adaptive Estimation	25
Figure 2.23 Quadratic Mean Filter Sensor Performance	27
Figure 3.1 Pick-Up Truck Based Water Spray System.....	28
Figure 3.2 Ice Patch Formation.....	29
Figure 3.3 Test Road.....	29
Figure 3.4 Measurement Data, Estimated Friction Coefficient	30
Figure 3.5 Applicator Control Signal.....	31
Figure 3.6 Test Road in the Map	31
Figure 3.7 Ice Patches Locations on the Test Road	32
Figure 3.8 GPS Receiver.....	32
Figure 3.9 Black Ice	33
Figure 3.10 Wet Road Comparison	33
Figure 3.11 Black Ice Data and Wet Road Measurement Data	34
Figure 3.12 Conventional Applicator	35
Figure 3.13 Zero Velocity Applicator.....	36
Figure 3.14 Setup for the Applicator Delay Measurement.....	37
Figure 3.15 Location of the Wooden Block.....	38
Figure 3.16 Wire Piece/Pylon Couple	38
Figure 3.17 Conventional Applicator Delay	39
Figure 3.18 Low Friction Plastic Surface	40
Figure 3.19 Filtering Algorithm Time Delay.....	41
Figure 3.20 Overall System Performance	42
Figure 3.21 First User Interface Screen	43

Figure 3.22 User Interface for Map Creation Software	43
Figure 3.23 Use of Map Creation Software	44
Figure 3.24 Road Map Displayed During Automatic Applicator Control.....	44
Figure 3.25 Friction Measurement System Installed on Pick-Up Truck	46
Figure 3.26 Microprocessor Enclosure Dimensions.....	46
Figure 3.27 Interface Ports on Microprocessor.....	47
Figure 3.28 Video Card and LCD Display	47
Figure 3.29 Microprocessor and Its Input-Output Interfaces.....	48

Executive Summary

This project focuses on the development and experimental evaluation of a tire-road friction measurement system and on the use of this measurement system for closed-loop applicator control on a snowplow. The friction measurement utilizes a small instrumented wheel on the vehicle. Unlike other systems previously documented in the literature, the developed system can provide a continuous measurement of the friction coefficient under all vehicle maneuvers, even when the longitudinal and lateral accelerations are both zero.

A key challenge in the development of the friction measurement system is the need to remove the influence of vibrations and the influence of vehicle maneuvers from the measured signal of a force sensor. An adaptive feedforward algorithm based on the use of accelerometer signals as reference inputs was developed. The parameters of the feedforward model were estimated by the adaptive algorithm and serve to determine the friction coefficient. The influence of vibrations and of vehicle maneuvers was also removed.

Detailed experimental results are presented on a skid pad wherein the road surface changes from dry asphalt to ice. Results are presented at different speeds and with and without lateral and longitudinal maneuvers. Excellent performance is obtained in estimation of the friction coefficient. The performance of the adaptive feedforward algorithm is shown to be significantly superior to that of a simple cross-correlation based algorithm for friction estimation.

A closed-loop controller based on the use of the estimated tire-road friction coefficient is developed for the applicator of a snowplow. The closed-loop applicator automatically applies deicing material whenever an icy spot is detected on the road.

The complete closed-loop system consists of a GPS receiver to record vehicle location, the friction measurement wheel, a microprocessor, a LCD touch panel, and the interface to the Dickey John controller of the applicator. The tire-road friction measurement system itself is modular and contains two parts: the lower friction wheel and the upper mounting assembly. The lower friction wheel is common to all vehicle configurations while the upper assembly is tailored to the specific vehicle that needs to be instrumented. Two types of vehicles – a snowplow and a pick-up truck – were instrumented and evaluated in this project.

The GPS system enables recording of the vehicle location together with the measured friction coefficient. This enables friction coefficient to be recorded as a function of vehicle location along the entire route covered by a snowplow. Further, software is also developed in the project to enhance the developed automatic applicator control system with utilization of real-time data from a geographical information system. By measuring vehicle location, information is obtained from the geographical database on upcoming geometric road alignments, stop signs and known problematic segments of roadway. The applicator is turned on automatically to treat these road segments. The developed software also enables the snowplow operator (or supervisor) to create the initial geographical database in which the road segments to be treated can be specified.

The hardware time delays of the applicator actuator on the snowplow and the software time delay of the friction estimation algorithm are both determined experimentally and the zero velocity applicator based closed-loop system is shown to work reliably at speeds up to 25 mph.

At speeds up to 25 mph, the closed-loop system is able to cover any detected slippery surface with the deicing chemical right from the beginning of the slippery road surface.

Chapter 1. Introduction

1.1 Winter Road Maintenance

Winter road maintenance is a major economic and public safety issue of common concern in countries having lengthy winter seasons. US Federal Highway Administration reports that over 74% of the nation's roads are located in snowy regions, which receive more than five inches average snowfall annually and nearly 70% of the U.S. population lives in these snowy regions [7].

On average, state expenditures associated with winter road maintenance account for roughly 20% of Department of Transportation maintenance budgets. Highway agencies spend more than 2.3 billion dollars on snow and ice control operations annually. Harsh weather and road conditions also have consequences on economic productivity. Each year trucking companies or commercial vehicle operators lose an estimated 32.6 billion vehicle hours due to low visibility or slick pavement-related congestion in the nation's metropolitan areas. The estimated cost of the delays to trucking companies ranges from 2.2 billion dollars to 3.5 billion dollars annually [3], [7].

Weather-related crashes are those that occur in the presence of adverse weather such as rain, sleet, snow, fog. Due to the slick, wet, snowy, slushy or icy pavements, these crashes constitute a significant portion of all motor vehicle accidents. Each year, 197,300 crashes occur and 700 persons are killed just due to the icy road surface conditions. That is, nearly 13% of all weather-related crashes and 10% of all weather-related crash fatalities [3], [7].

Adverse weather and road conditions also affect mobility. Free-flow speed is the term used to describe the average speed at which a motorist would travel if there were no congestion. It has been estimated that snow can cause free-flow speed to decrease by a maximum of 64% and highway capacity to reduce by 12% to 27% [7].

Many highway agencies serving in the cold regions of the world have considered measurement of surface friction measurements to improve their winter maintenance operations and ameliorate the above mentioned statistics on winter maintenance cost, economic productivity, public safety and mobility for the benefit of society. Many highway agencies in Europe, Japan, and the U.S. have come to believe that surface friction measurements may form the basis for improved winter maintenance operations and mobility [4], [7].

Efficient use of deicing material, minimum environmental damage and reduced cost are the main goals for the design of an automated winter maintenance system. Measurement of tire-road friction coefficient provides information about the road surface condition. Then, the closed-loop control of the applicator based on these measurements optimizes the amount of deicing material that needs to be applied on the roadway, prevents the excessive use of chemicals and saves tax payer's money.

A snowplow operator must not only drive the snowplow truck under very difficult visibility conditions, but also control the snowplow blades to push the snow aside and must also control

the deicing applicator. Having an automatic feedback control based applicator will reduce the burden on the snowplow operator and make his/her job easier.

Operators mostly rely on visual inspection while deciding on whether the application of deicing material is necessary or not and often their decision is not accurate [4]. For example, in case of a snowstorm, visibility of the roadway may decrease significantly due to the blinding effect of the snow blowing; or an icy road surface may be covered by a thin layer of soft snow which makes the ice invisible from a distance; or a naked eye may not be able to differentiate black ice formation from the wetness of the road surface. Since the operator has no direct information about the slipperiness of the road surface, in order to be on the safe side, he/she usually tends to apply more chemicals than is actually needed. This argument is valid especially for new and inexperienced snowplow operators.

Excessive use of deicing materials increases the winter maintenance costs and also has a negative impact on environment by polluting lakes and rivers [1]. However, an impetuous attempt to minimize the deicing material consumption without using a reliable and objective criterion would also increase the risk of accidents. The proposed closed-loop control system basically eliminates this trade off and optimizes the use of deicing chemicals by measuring the road surface condition directly and generating an output signal to control the applicator in real-time based on these measurements.

The system described herein can also be adapted to existing winter road maintenance systems, such as the Maintenance Decision Support (MDS) system developed and used by Mn/DOT. The MDS system obtains measurements from a Road Weather Information System (RWIS) for winter road maintenance. RWIS utilizes environmental sensor stations to measure data on road pavement and atmospheric weather conditions. Data gathered from a series of in-pavement sensors, sub-surface probes and meteorological equipment are combined with weather forecast to predict pavement surface conditions up to 12 hours in advance. Highway winter road maintenance managers then use RWIS data to make decisions on anti-icing treatments for roads as well as for scheduling of snow plowing operations. While RWIS measurements help provide *anti-icing* treatment for roads and prevent ice formation in certain situations, they do not help with *deicing* treatment. The friction measurement system developed in this project on the other hand, is useful for real-time decisions on *deicing* treatment of roads by real-time control of the applicator on each snowplow.

The developed system can thus augment existing systems which are based on use of RWIS data and improve their performance.

1.2 Review of Friction Measurement Systems

Many friction estimation systems have previously been proposed in literature which can be classified into three main groups, namely vehicle based, wheel based and tire based systems [2].

a) Vehicle Based Systems

Vehicle based systems utilize the lateral and longitudinal motions of the vehicle to estimate the friction coefficient [6]. The slip angle is measured by means of a gyroscope, lateral accelerometer and a steering angle sensor while the measurement of slip ratio requires the use of

wheel speed sensors. A GPS receiver is also employed in both lateral and longitudinal control systems to measure the magnitude and the orientation of the vehicle's velocity vector defined in the inertial frame. A differential GPS system, which is expensive and only available in some geographic locations, is necessary for high accuracies. A real-time parameter identification algorithm is utilized to obtain the real-time tire-road friction estimate. The vehicle based system works during acceleration and deceleration of the vehicle and can work over a large range of slip values. However, the vehicle needs to be either accelerating or decelerating or cornering in order for the friction estimation algorithm to work and update the friction coefficient estimates. The vehicle based friction estimation algorithms do not work when there is no acceleration, deceleration or cornering [6].

b) Wheel Based Systems

This type of measurement system utilizes a redundant wheel and is appropriate for heavy duty trucks such as snowplows. The Norse meter is a commercialized wheel based system which is used in winter road maintenance. This system requires a dedicated operator and a brake actuator to skid the additional wheel on the roadway at timed intervals. The Norse meter is described further in the following chapter. The wheel based system designed at the University of Minnesota and described herein has several advantages over this traditional Norse meter system.

This project describes the University of Minnesota wheel based friction estimation system in detail. The developed system employs an additional wheel which is at an angle with the traveling direction of the snowplow. The angle, namely the slip angle, generates a continuous lateral force even in the absence of cornering. The continuous force signal enables the design of an autonomous applicator control system which is very beneficial for the effective maintenance of the roadways. The measured lateral force signal is filtered and processed in real time with the help of some novel algorithms developed for accurately estimating the tire-road friction coefficient. The road surface condition is precisely evaluated with the tire-road friction coefficient and a control signal is sent to the applicator with respect to the output of a change detection algorithm.

c) Tire Based Systems

Tire based systems [2], [6] utilize the direct measurement of elastic tire deformations to estimate the tire-road friction coefficient. There are various types of tire based systems under development, employing different measurement technologies. However, none of these technologies are mature and reliable enough to be adapted for closed-loop applicator control.

1.3 Project Contributions

A wheel based friction measurement system is developed for the closed-loop control of snowplow applicators that can work reliably up to a truck speed of 25 mph in real-time. This system:

- Measures the friction coefficient of the road pavement continuously,
- Detects any road surface condition change quickly,
- Activates/deactivates the snowplow applicator accordingly, and

- Applies chemicals or deicing materials on the road surface effectively.

From a technical point of view, the main contribution of this part of the work is the development of several vibration cancellation algorithms for the removal of excessive vibrations on the measured force signal. This is basically the fundamental challenge in the design of a real-time automated friction measurement system since the excessive vibrations mask the change in friction coefficient and slow down the friction change detection. The developed algorithms include:

- Cross-Correlation Based Vibration Cancellation
- Adaptive Feed-Forward Filter for Vibration Cancellation
- Biased Quadratic Mean Filter

The first two algorithms are based on the use of an auxiliary accelerometer whereas the last one is based on the inherent statistical characteristic of the measured force signal particular to snowplow application. In addition, the influence of steering maneuvers and longitudinal acceleration/deceleration maneuvers are removed by using the same acceleration based cancellation algorithms.

The closed-loop applicator control system is enhanced by using a geographical information system that utilizes stored information on road pavement locations that need to be treated by the applicator. This pavement treatment is in addition to the treatment based on measured tire-road friction coefficient. A GPS unit measures vehicle location which is then utilized to access a geographical information system that updates road locations to be treated and automatically controls the applicator.

A description of the hardware and software developed is provided in section 3.7 of this report. The developed hardware is compact and modular.

Tests are carried out for the evaluation of both the performance of the friction measurement system as well as the closed-loop applicator control system, including measurement of hardware and software time delays, differentiation of black ice and wet road, ability of the applicator to cover detected ice at different snowplow speeds, and mapping of the road friction coefficient as a function of location using a GPS unit.

Chapter 2. Friction Measurement System and Its Evaluation

2.1 Conventional Friction Estimation Method

The Norse meter is a wheel-based friction measurement system that overcomes the primary disadvantage of the vehicle-based estimation methods. It can estimate the friction coefficient under all vehicle maneuvers (or the absence of maneuvers). The Norse meter consists of an external redundant wheel fixed to the vehicle. The redundant wheel is instrumented with force-measurement load cells and also contains a hydraulic brake actuator that can apply brake torque to the redundant wheel. The technique behind the Norse meter is to intermittently apply a controlled braking torque to the redundant wheel until the tire starts to skid and high slip ratios are created at the contact patch. Under very high slip ratios, the ratio of longitudinal tire force to vertical tire force is proportional to the tire-road friction coefficient. Thus, by measuring vertical and longitudinal tire forces at high slip ratios, the friction coefficient is calculated. The picture of the Norse meter is presented in Figure 2.1.



Figure 2.1 Photograph of the Norse Meter

However, the Norse meter has several disadvantages. First of all it only works intermittently by applying brake torque whenever it is required to measure the friction coefficient. It does not provide a continuous measurement of friction coefficient. Furthermore, due to the use of hydraulic equipment, brake actuators and multiple load cells, it is expensive (over \$50,000) and prone to frequent breakdown. The use of many moving parts and frequent braking causes tire wear as well as breakdown of other components requiring frequent maintenance.

2.2 Advantages of New Wheel Based System

The new wheel based friction coefficient measurement system developed at the University of Minnesota is a wheel based system like the Norse meter, but overcomes many of the disadvantages of the Norse meter.

The new wheel based system has minimal moving parts and does not require the application of braking for friction measurement. Instead it works by continuously measuring the lateral tire force. It is not an intermittent system like Norse meter meaning that it provides a continuous

estimation of the friction coefficient. Furthermore, it is simpler and less expensive than the commercially available Norse meter system. The new friction measurement system also works under all vehicle maneuvers or the absence of vehicle maneuvers.

2.3 New Wheel Based Friction Estimation System

The road surface condition data is measured through an additional wheel mounted between the front wheels of the snowplow. The wheel is driven by traction forces, i.e. no active drive torque applies to the wheel. A load cell, which is positioned between the truck and the wheel system, measures the lateral tire forces acting on the wheel along with the vibrations coming from the roadway. Measurements are then filtered and processed by a microprocessor that generates an output signal to control the deicing applicator at the back of the snowplow. The locations of the additional wheel and the applicator are shown on a snowplow in Figure 2.2. The friction wheel can be placed at a lateral location corresponding to a wheel path of a standard passenger car. It is also possible to have two friction wheels installed on the snowplow so as to measure the friction coefficient at lateral locations corresponding to both wheel paths of passenger vehicles.

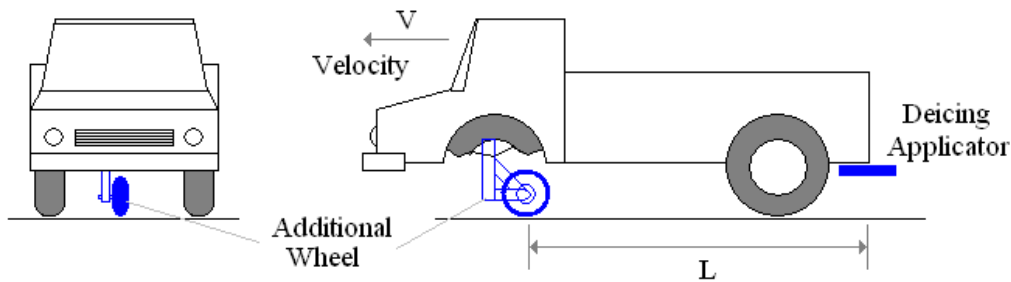


Figure 2.2 Winter Road Maintenance System

2.4 Design Constraints

The system needs to operate in real-time, since a real-time system guarantees that a slippery part detected on the road surface by the additional wheel is treated properly with the deicing material deployed by the applicator. Hence, only a limited time is available for processing the data, estimating the friction coefficient and generating an appropriate control signal for the deicing applicator.

The available time can be defined as in Equation (2.1) where V is the speed of the snowplow and L is the longitudinal distance from the redundant wheel at the front to the applicator at the back.

$$T_{available} = L/V \quad (2.1)$$

In other words, once the additional wheel goes over a slippery surface transition, the data processing unit has a total time of T seconds to detect the change and send a control signal to the applicator.

Truck Speed [mph]	Available Time [msec]
20	671
30	447
40	336
50	268

Table 2.1 Truck Speeds vs. Available Times for Data Processing and Applicator Activation

Various snowplowing speeds and corresponding available times are listed in Table 2.1 for a truck having a longitudinal distance of approximately 6 meters from the wheel to the applicator. The minimum available time occurs at the highest snowplowing speed and the main goal is to keep the data processing time less than the minimum available time.

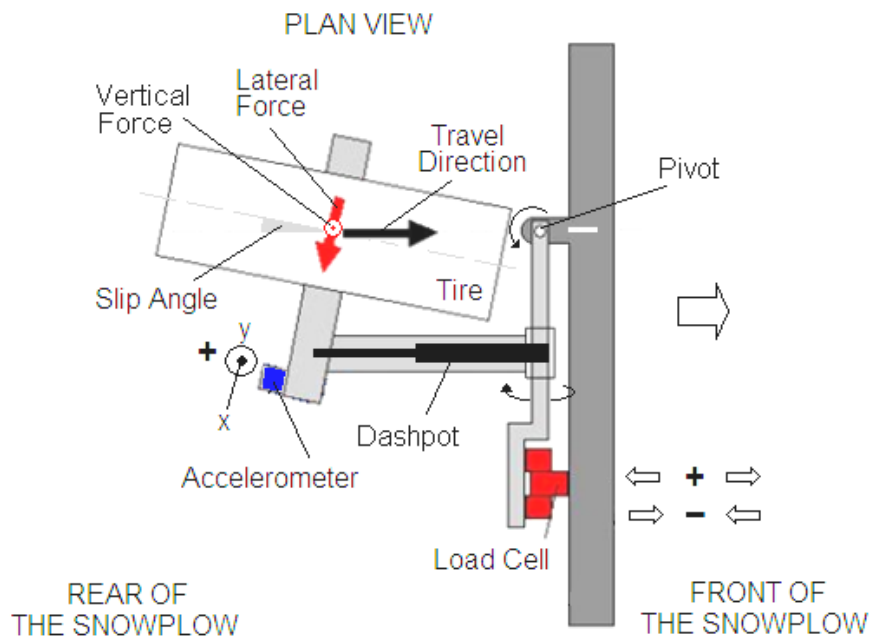


Figure 2.3 Plan View Schematic of the Wheel Based System

2.5 Friction Coefficient Measurement System

The plan view schematic of the developed friction measurement system is presented in Figure 2.3. The friction wheel is attached to the truck chassis through a hinge having a vertical pivot axis and the load cell. The equatorial line of the tire makes an angle with the traveling direction of the truck. The constant angle, which is also known as the slip angle α_0 , introduces a

continuous lateral tire force F_{Lat} at the center of the tire contact patch. The photograph of the system is also given in Figure 2.4.



Figure 2.4 Photograph of the Wheel Based System

The static vertical force on the tire is kept constant using a pneumatic actuator, air supply from the available compressed air cylinder on the truck and a pressure servo loop. The lateral tire force for a given tire typically depends on the vertical tire force F_z , on the slip angle α and on the tire-road friction coefficient μ . If vertical tire force is assumed to be constant and if the slip angle α is assumed to be large enough, then the lateral tire force reaches its maximum value which is given by Equation (2.2):

$$F_{Lat}(\alpha_0) = \mu \times F \quad (2.2)$$

Since the vertical tire force is kept constant in the developed sensor system and the slip angle α is fixed to a value high enough, i.e. $\alpha_0 \cong 6^\circ$, the lateral tire force F_{Lat} is assumed to be proportional to the tire-road friction coefficient. One can simply determine the tire-road friction coefficient in real time by just measuring the lateral tire force signal and dividing it by the constant vertical tire force. However, if the vertical tire force is assumed to be constant, then the lateral tire force contains all the necessary information for detecting a surface change on the roadway. Hence the friction coefficient can be determined by measuring the lateral tire force and scaling this value appropriately.

It should be noted that the pneumatic servo loop only has a low bandwidth of around 0.1 Hz. Thus it can only maintain a constant “static” vertical tire force. Variations in vertical tire force that happen due to maneuvers such as acceleration and/or cornering and due to vibrations induced by the road cannot be compensated by the pneumatic actuator. It should also be noted that a slip angle of 6° is high enough to ensure that the lateral force changes with friction coefficient. For very small slip angles of 1° or 2° , the lateral force may not change significantly with friction coefficient and may be measured to be about the same value for all friction coefficients.

A pancake type load cell is used to measure the lateral tire force and an inexpensive MEMS accelerometer is employed to detect the vibrations and filter out the noise on the force signal. The total cost of material, electrical supplies and sensors for the developed friction measurement

system is less than \$1500. This includes the cost of both the computer system and the load cell which constitute the two most expensive components of the system.

2.6 Technical Challenges

a) Influence of Vibrations

The fundamental technical challenge in the design of a wheel based tire-road friction coefficient estimation system is the enormous noise on the force signal which is mainly caused by the excitations coming from the roadway. Two frequency bands, which are centered at about 1-2 Hz and 10Hz, stick out in the frequency spectrum of a typical force signal as shown in Figure 2.5. The static component (~ 0 Hz) of the frequency spectrum plot corresponds to the steady state lateral force which provides the friction coefficient information.

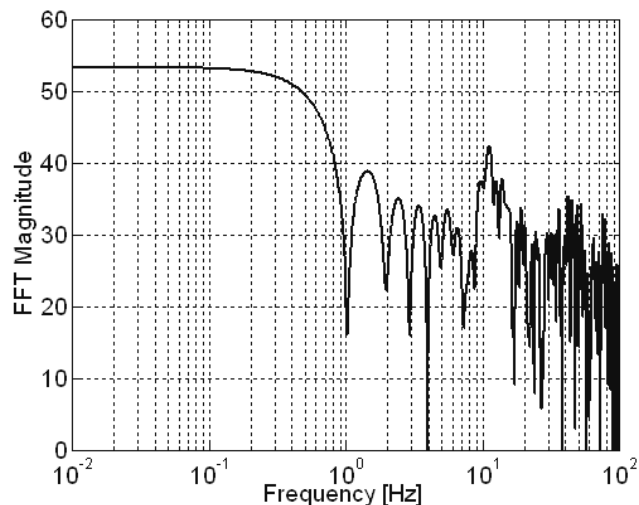


Figure 2.5 Frequency Spectrum of a Typical Force Signal

Although, high frequency bands (>5 Hz) of the noise contain substantial amount of energy, it is quite feasible to design a linear low pass filter and remove this portion of the noise within acceptable time limits. However, filtering out the low frequency content (<1 Hz) of the noise within the same time limits is much more difficult. Since only a limited amount of noise reduction can be achieved within the given minimum available time, the low frequency content continues to interfere with step changes in the force signal and hinders reliable detection of road surface changes.

Figure 2.6 shows a typical load cell measurement before and after filtering out the high frequency components using a second order Butterworth filter having a cut-off frequency of 5 Hz. The measurement is taken while the truck travels at a speed of 30 [mph] on a roadway having a surface transition from asphalt to ice. It can be seen that the filtered signal still has significant noise that remains, mostly at lower frequencies, between 1 – 5 Hz.

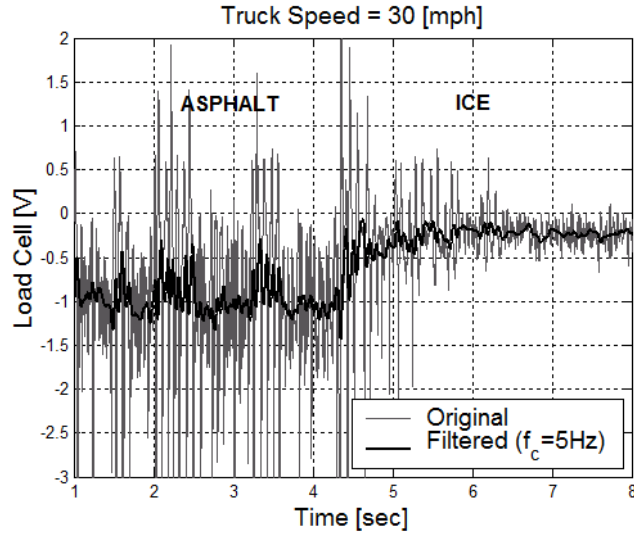


Figure 2.6 Typical Load-Cell Signals Before and After Low Pass Filtering ($f_c=5\text{Hz}$)

It is also possible to use a low pass filter having a much lower cut-off frequency, such as 0.5 Hz. However, such a filter has a longer response time and thus violates the minimum available time constraint of the real-time system when an abrupt change occurs in the lateral force signal due to the tire-road friction coefficient change, as shown in Figure 2.7.

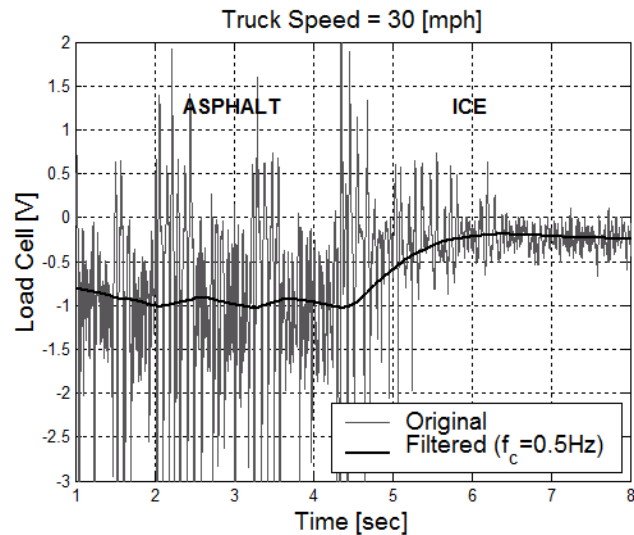


Figure 2.7 Typical Load-Cell Signals Before and After Low Pass Filtering ($f_c=0.5\text{ Hz}$)

Thus, a primary challenge is to design estimation and filtering system that can quickly filter out the excessive noise, especially in the low frequency bands, while preserving the quick step changes that occur due to different road surface conditions.

b) Influence of Vehicle Maneuvers

In order to measure the lateral force on the tire used in the friction measurement system, first the effects of longitudinal tire forces and the variations in lateral tire forces due to steering

maneuvers should be eliminated. Longitudinal tire force occurs due to the acceleration and deceleration of the truck. In the developed system, the center of the tire-road contact patch is aligned with the vertical pivot axis so that the effect of longitudinal force on the reading of the load cell is eliminated by design. However, steering maneuvers give rise to significant variations in the measured lateral force. An algorithm that can remove the influence of these steering maneuvers so as to enable friction estimation during cornering is therefore also required.

2.7 Correlation of Force and Acceleration Signals

In order to measure vertical acceleration experienced by the friction wheel, an accelerometer is mounted at the center of the additional wheel, as shown in Figure 2.8.

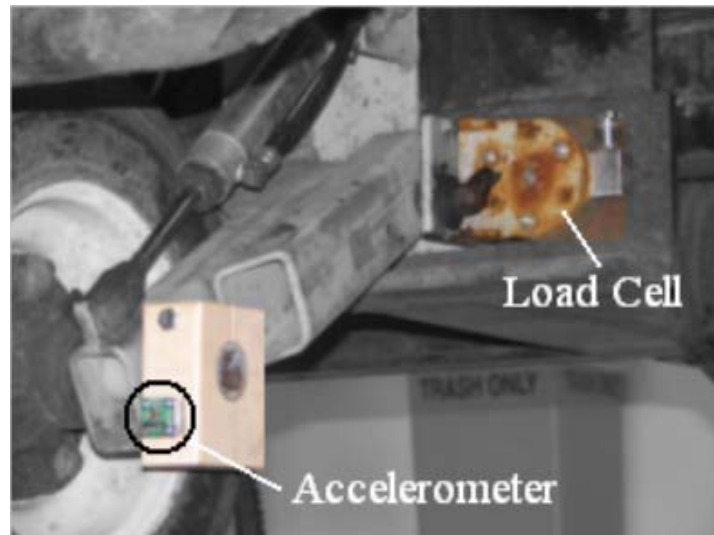


Figure 2.8 Accelerometer and Load Cell Locations

This accelerometer measures only the vertical vibrations coming from the roadway while being indifferent to the step changes in the lateral force signal that occur due to the road surface friction coefficient changes. The developed vibration cancellation algorithms exploits this property of the accelerometer signal to remove the low frequency noise on the force signal.

From a large set of conducted measurements, the vertical acceleration signal and the disturbances on the measured force signal are observed to be highly correlated. Figure 2.9 shows the load-cell signal along with the vertical accelerometer signal from one sample data set. The accelerometer, which is mounted close to the center of the wheel, measures the vertical vibrations of the redundant wheel while being neutral to road surface friction coefficient transitions. These vibrations are then transmitted through the chassis of the wheel system to the load-cell where they cause similar disturbances on the force signal, but in smaller relative magnitude scales. In the measurements, the acceleration signal also consistently leads the disturbance signal with a time delay which implies causality between the two signals as shown in Figure 2.10.

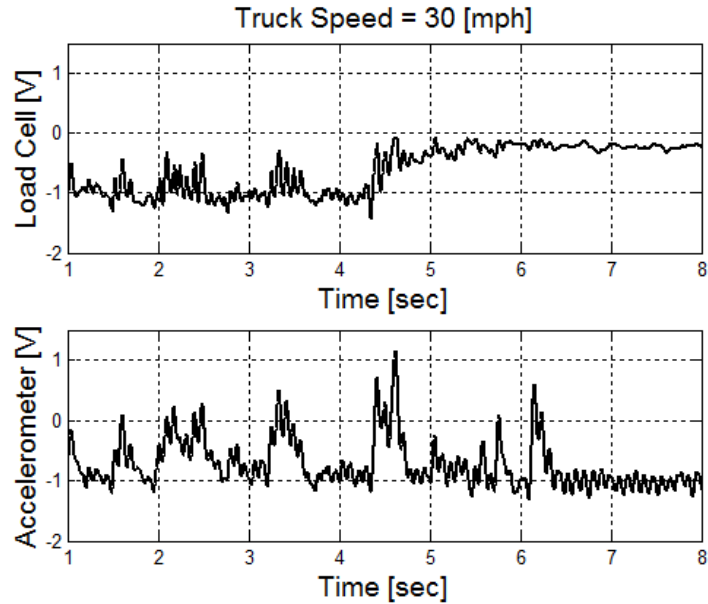


Figure 2.9 Low Pass Filtered Load-Cell and Acceleration Signals ($f_c=10\text{Hz}$)

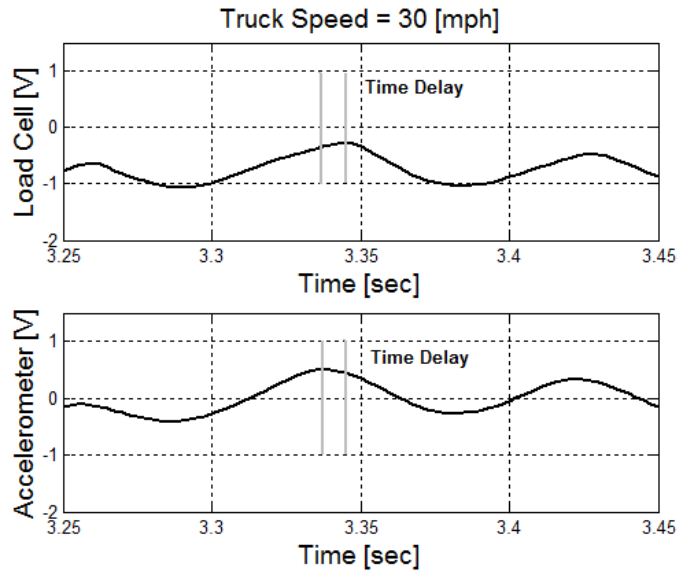


Figure 2.10 Time Delay between the Load-Cell and Accelerometer Signals

Thus, there is a high correlation between the accelerometer and load cell signals. In order to remove low frequency content of the noise, a cross-correlation based algorithm or a special adaptive filter can be formulated. The following section focuses on the cross-correlation based algorithm.

2.8 Cross-Correlation Based Vibration Cancellation

First, the high frequency contents of both the force and the accelerometer signals are filtered out by means of a traditional low pass filter. Next, in order to enhance the correlation coefficient by shifting the force signal with respect to the accelerometer signal the time delay between these

two signals need to be known. Since the time delay between the force and the accelerometer is observed to change slightly and occurs in a limited time span, it is possible to develop an algorithm as described in the following steps that seeks for the time delay yielding the maximum correlation coefficient.

- Predefine a set of delays (time-step in discrete time) as in Equation (2.3).

$$P = \{-3, -2, -1, 0, 1, 2, 3\} \quad (2.3)$$

- Shift the accelerometer signal as much as the time delays in the set.
- Calculate the correlation coefficient between the force and the shifted accelerometer signals for each and every time delay in the set P.

$$C_{yf}(p) = \frac{\sigma_{yf}(p)}{\sqrt{\sigma_{yy} \sigma_{ff}}} \quad (2.4)$$

Here p refers to the current time delay selected from the set P , $C_{yf}(p)$ is the correlation coefficient and $\sigma_{yf}(p)$ the covariance function between the shifted accelerometer and force signals, and $\sigma_{yy}(p)$ and $\sigma_{ff}(p)$ are the variances of the shifted accelerometer and force signals respectively.

- Find the time delay yielding the maximum correlation coefficient.

$$\bar{p} = \{p : p \in P \ \& \ C_{yf}(p) = \max[C_{yf}(p)]\} \quad (2.5)$$

- Repeat the steps for the next time window as the time window moves forward in time.

Finally, the shifted version of the accelerometer signal is scaled with a constant determined experimentally on asphalt road and added to the load cell signal in order to cancel out the low frequency noise on the force signal. This algorithm uses a constant scale factor for simplicity. However this is a serious drawback of this algorithm when compared with the adaptive filter discussed in the following section.

2.9 Adaptive Feed-Forward Filter for Vibration Cancellation

Next, an effective adaptive vibration cancellation algorithm is developed to remove the influence of vibrations from the lateral force signal. The adaptive parameters of the feedforward model used in the vibration cancellation system serve to identify the tire-road friction coefficient rapidly in real-time.

A schematic of the estimation system using this approach is shown in Figure 2.11. The vibrations come from road induced excitation or from other vibration sources existing in the vehicle. These vibrations constitute the disturbances that act on the system. The measurement of the disturbances at the source is not possible. However, as a substitute for this the vertical acceleration is measured using an accelerometer mounted at the center of the wheel as shown in Figure 2.8. The transfer function between the source of disturbances and the lateral force input to the wheel is $G(z)$ where as the transfer function between the disturbance and accelerometer signal is $H(z)$.

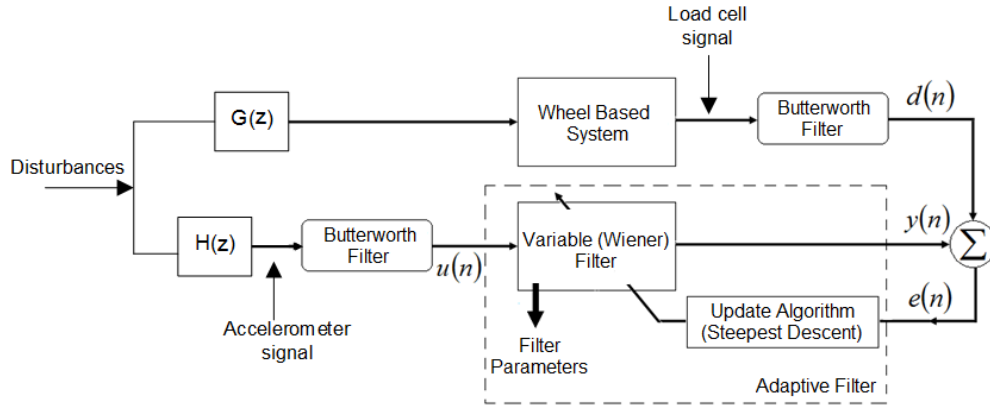


Figure 2.11 Block Diagram of Proposed Estimation Algorithm

Accelerometer and load cell signals are first filtered with a Butterworth filter with a corner frequency of 5 Hz to remove high frequency noise. The filtered load cell signal is denoted by $d(n)$ while the filtered accelerometer signal is denoted by $u(n)$. There is an unknown steady state relationship between u and d and a Wiener filter is used to represent this unknown relationship:

$$y(n) = \sum h_{\ell} u(n - \ell) \quad (2.6)$$

The order of the filter used in the estimations is four. The coefficients of the filter are identified in real time using an adaptive estimation algorithm. At steady state, $y(n)$ should converge to $-d(n)$, after convergence of the adaptive parameters h_1 .

Note also that the filter parameters depend on friction coefficient μ . Vertical vibration of the redundant wheel causes variation in the normal force between the tire and the ground. This in turn causes a change in the lateral force read by the load cell. The lateral force is a function of both μ and F_z , since $F_{Lat} = \mu F_z$ for large slip angle.

The error between the desired output and the actual filter output is defined as in Equation (2.7).

$$e(n) = d(n) - y(n) \quad (2.7)$$

And the error square is defined as in Equation (2.8).

$$\xi(n) = e^2(n) \quad (2.8)$$

Then the gradient of $\xi(n)$ wrt the filter parameters h_1 is defined as in Equation (2.9)

$$\nabla \xi(n) = 2[\nabla e(n)]e(n) \quad (2.9)$$

The error $e(n)$ can be rewritten as in Equation (2.10)

$$e(n) = d(n) - \sum_{\ell} h_{\ell}(n)u(n - \ell) \quad (2.10)$$

by substituting Equation (2.6) into Equation (2.7). Hence the gradient of the error is calculated as in Equation (2.11).

$$\nabla e(n) = \left[\frac{\partial e}{\partial h_1} \quad \frac{\partial e}{\partial h_2} \quad \dots \quad \dots \quad \frac{\partial e}{\partial h_m} \right]^T \quad (2.11)$$

Equation (2.13) follows the relationship in Equation (2.12).

$$\frac{\partial e_i}{\partial h_i} = u_i \quad (2.12)$$

$$\nabla e(n) = [u(n) \quad u(n-1) \quad \dots \quad \dots \quad u(n-m)]^T \quad (2.13)$$

The adaptive algorithm updates the filter parameters as in Equation (2.14) in the direction of the gradient $\nabla e(n)$ using the step size parameter, ρ which is selected as 0.005.

$$\begin{bmatrix} h_1(n) \\ h_2(n) \\ \vdots \\ \vdots \\ h_m(n) \end{bmatrix} = \begin{bmatrix} h_1(n-1) \\ h_2(n-1) \\ \vdots \\ \vdots \\ h_m(n-1) \end{bmatrix} + \rho \begin{bmatrix} u(n) \\ u(n-1) \\ \vdots \\ \vdots \\ u(n-m) \end{bmatrix} e(n) \quad (2.14)$$

When the friction coefficient μ is constant (for example, 0.9 on a dry asphalt road), the parameters h_1 will converge to constant values. These constant values will be such that the error $e(n)$ will be approximately zero. However, when the friction coefficient μ changes, new parameters will have to be found that make $e(n)$ zero. This is because the vibrations influence the lateral force F_y with a different scaling factor for a different value of μ . By keeping track of the changes in the parameters h_i , the friction coefficient μ can be obtained in real-time. The relationship between the friction coefficient and the first filter parameter h_0 can be defined as given in Equation (2.15)

$$\mu = -a * (h_0 + b) \quad (2.15)$$

where a and b values are chosen such that the friction coefficients of asphalt and ice map to the levels reported in the literature which are in the ranges of 0.8–0.9 and 0.1–0.3, respectively. Hence adaptive estimation of the parameter h_0 provides the real-time value of the friction coefficient μ .

It should be noted that the output of the adaptive filter $y(n)$ after convergence of the filter parameters is a replica of the measured force and thus cannot by itself provide the friction coefficient.

2.10 Change Detection Algorithm

Detection of the change in friction coefficient is made based on a change in the value of the parameters of the filter used in the adaptive feedforward vibration cancellation algorithm. This change in parameter value is detected using a likelihood ratio based change detection algorithm.

Likelihood is defined as the probability of the data being the same as the observed data set (y), given the probability density distribution. If the probability density distribution model is assumed to be a Gaussian distribution, the likelihood function can be calculated as the product of the probability density of each sample as in Equation (2.16).

$$p(y|\theta) = l(\theta|y) = \prod_{i=1}^N \frac{1}{\sqrt{2\pi\sigma^2}} e^{-\frac{1}{2}\left(\frac{y_i - \bar{y}}{\sigma}\right)^2} \quad (2.16)$$

The maximum likelihood estimator (MLE) yields the distribution parameter vector (θ) which maximizes the likelihood function. For a Gaussian distribution, the distribution parameter vector maximizing the likelihood function consists of mean and variance of the distribution. The output vector of the developed algorithms, having the same size as the moving time window (N), corresponds to the observed data in our case. The observed data set in a moving time window is assumed to have a Gaussian distribution; therefore the moving mean and the moving standard deviation of the data set are determined.

The likelihood-ratio test statistic is the ratio between the likelihood evaluated at the MLE and the MLE subject to a restrictive parameter vector (θ_r) as in Equation (2.17).

$$\Lambda = 2 \ln \left\{ \frac{l(\theta | y)}{l(\theta_r | y)} \right\} = -2 \ln \left\{ \frac{l(\theta_r | y)}{l(\theta | y)} \right\} = -2 \{L(\theta_r | y) - L(\theta | y)\} \quad (2.17)$$

The restrictive parameter vector can be chosen based on an extremum level of the friction coefficient, so that the deviations from this level yield a significant step change in likelihood ratio (Λ). In the current design, the restrictive parameter vector can be chosen with respect to the minimum/maximum expected level of the friction coefficient. Next, a hypothesis test is applied to the likelihood ratio, meaning that a certain threshold is chosen, considering the anticipated friction coefficient range. If the threshold is exceeded, a control signal is sent to the deicing applicator. Using this detection algorithm will be much more meaningful when there is substantial amount of measurement data taken by different snowplows at different times and locations. For a single road, measurements are quite repeatable so that a threshold can be selected after a couple of runs.

2.11 Experimental Results

A large number of tests have been conducted to evaluate the performance of the designed friction coefficient estimation system. These include

- a) testing the algorithm on a skid-pad having a surface transition from dry asphalt to ice, at different snowplow speeds.
- b) examining the effects of acceleration, deceleration and steering maneuvers on the measurement system

This section focuses on the skid pad tests.



Figure 2.12 Skid-Pad Test Environments

The test environment is a special, closed-to-traffic roadway with a length of approximately 0.5 km. The first two thirds of the road surface is dry asphalt, while the rest is covered with hard ice. The transition from dry asphalt to icy road does not occur abruptly; rather it occurs gradually through a road surface composed of a mixture of wet asphalt and soft ice, as shown in Figure 2.12.

The lateral tire forces and the estimated tire-road friction coefficients at two different snowplow speeds are presented in Figure 2.13, Figure 2.14, Figure 2.15 and Figure 2.16. The speeds which range from 20 [mph] to 40 [mph], cover the speed range in which the snowplows operate during a snowstorm in real-life.

Figure 2.17 and Figure 2.18 compare the performance of the developed vibration cancellation system with an ordinary low pass filter at vehicle speeds of 30 and 35 [mph]. The cut-off frequency of this low pass filter is picked such that the noise levels are in the same order of magnitude as the noise levels of the adaptive system.

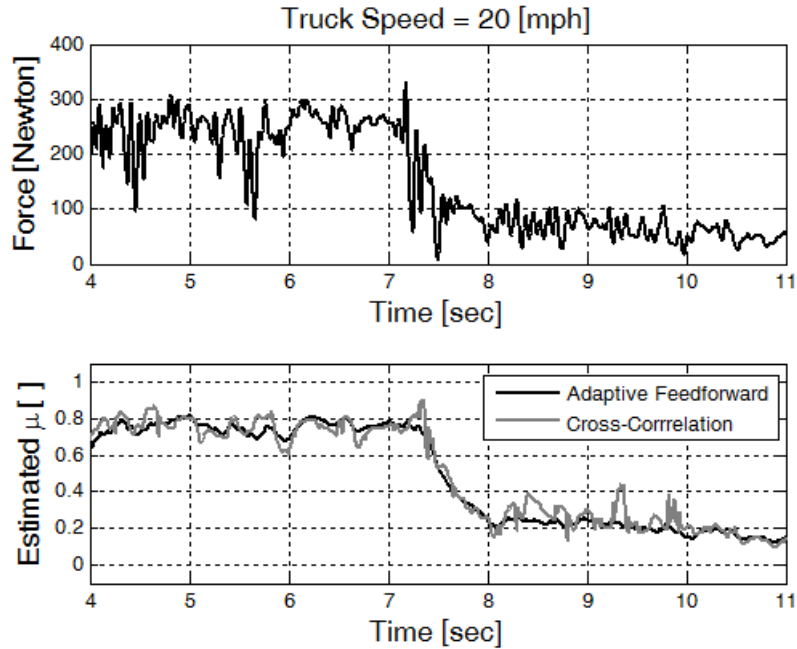


Figure 2.13 Tire-Road Friction Coefficient Estimation at 20 mph

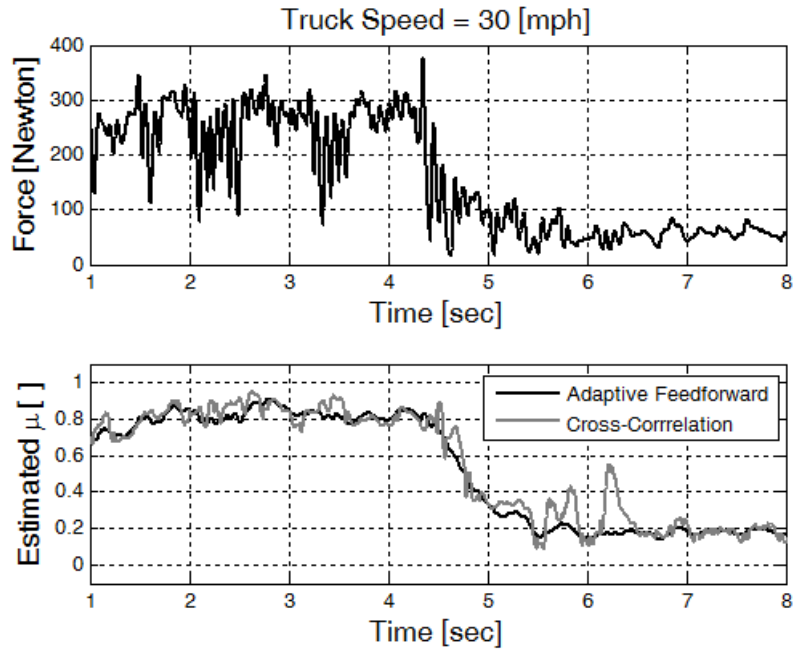


Figure 2.14 Tire-Road Friction Coefficient Estimation at 30 mph

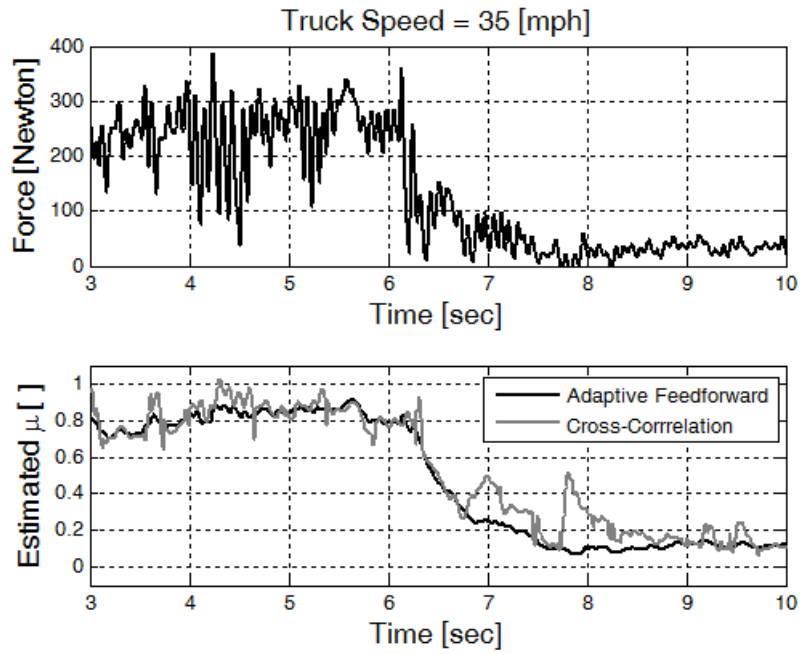


Figure 2.15 Tire-Road Friction Coefficient Estimation at 35 mph

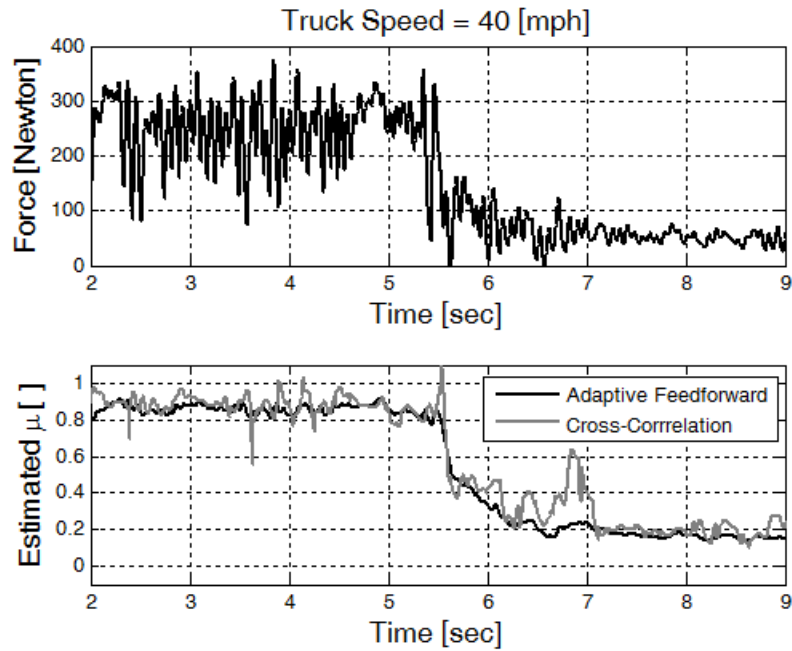


Figure 2.16 Tire-Road Friction Coefficient Estimation at 40 mph

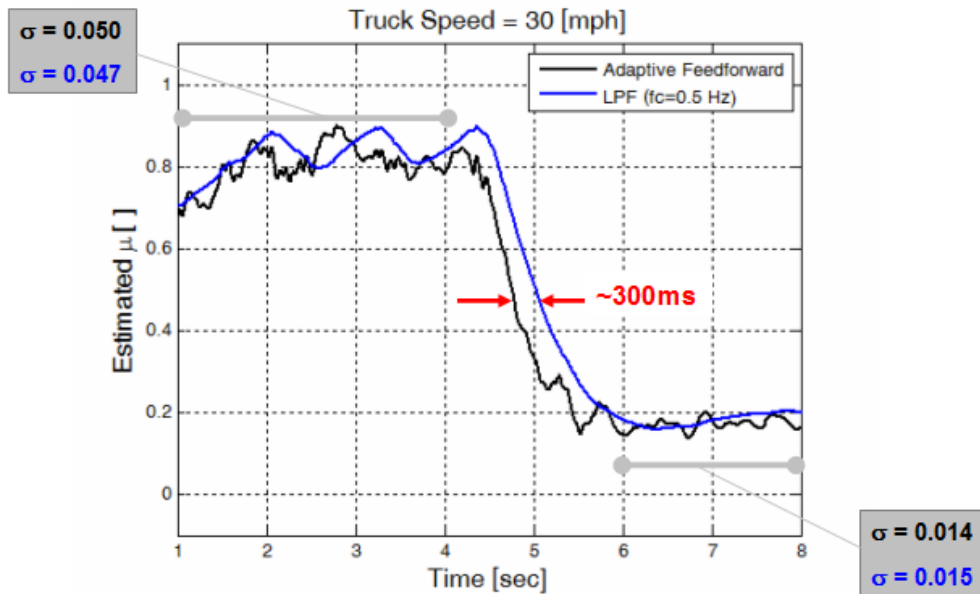


Figure 2.17 Adaptive Feedforward vs. Traditional LPF at 30 mph

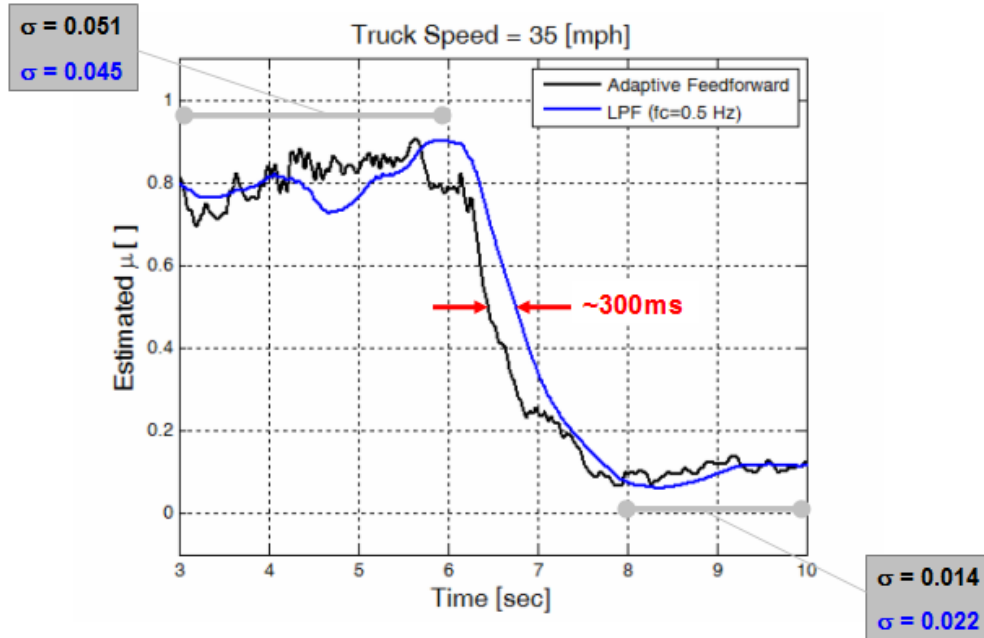


Figure 2.18 Adaptive Feedforward vs. Traditional LPF at 35 mph

From the experimental data presented above, the following conclusions can be drawn:

1. The noise on the force signal $d(n)$ is high and masks the change in the friction coefficient value μ .
2. The noise due to vibrations increases gradually as the snowplow speed increases.
3. Both the adaptive feedforward based vibration cancellation algorithm and the simple cross-correlation based algorithm are effective at removing most of the low frequency vibrations from the load cell signal.
4. The adaptive feedforward algorithm performs significantly better than the cross-correlation algorithm in removing vibrations. This difference in performance can be seen clearly, for example, during the transition from dry asphalt to ice.
5. After the transition to ice, the cross-correlation based vibration algorithm experiences a significant vibration due to a bump in the road. The effect of this bump can be seen at around 7th second in Figure 2.16. Since the scaling factor for the cross-correlation based algorithm is selected based on dry asphalt measurements, the algorithm is not able to perform well on ice. The adaptive feedforward algorithm, on the other hand, performs extremely well in being able to remove the vibrations due to the bump on the icy road. It can perform well on both dry asphalt and icy road.
6. A traditional low pass filter having the same noise reduction performance causes 300 [msec] more time delay compared to the adaptive algorithm.

2.12 Cancellation of Vehicle Maneuvers

a) Effects of Acceleration and Deceleration

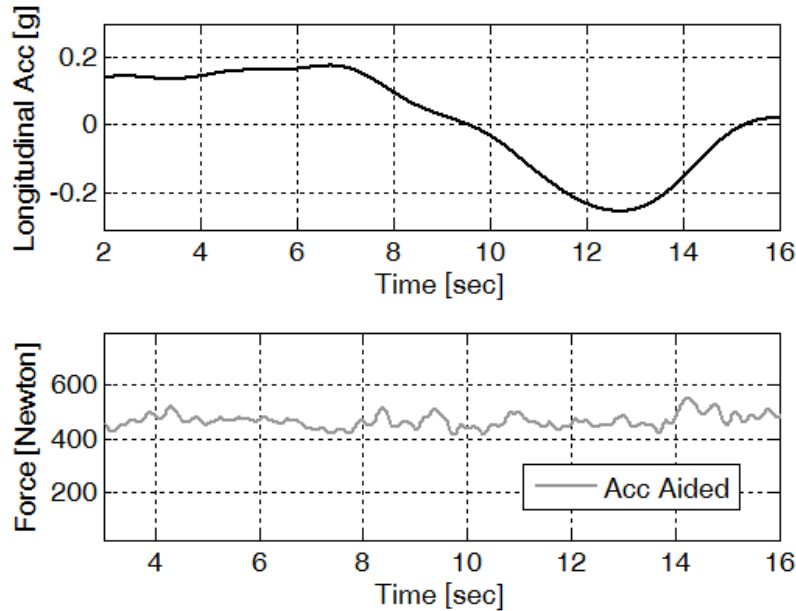


Figure 2.19 Effect of Acceleration and Deceleration of the Snowplow

The longitudinal force at the contact patch is not measured by the load cell since the center of the contact patch is aligned with the vertical hinge. This also means that the longitudinal acceleration and deceleration of the snowplow should not have any effect on the load cell measurements. This is shown in the experimental data given in Figure 2.19.

A stationary snowplow is accelerated from zero to a maximum velocity (30mph), and then decelerated back to zero velocity and brought to a complete stop. The longitudinal acceleration of the redundant wheel is measured with the help of another accelerometer. The measured force signal is not affected by the acceleration changes as seen in the lower portion of the figure.

b) Cancellation of Lateral Vehicle Maneuvers

The steering of the snowplow also contributes to the lateral force and the effect of steering can be eliminated by using an adaptive cancellation algorithm with the help of a steering angle sensor or a lateral accelerometer. In the current version of the system, a lateral accelerometer is used to compensate for the steering effect.

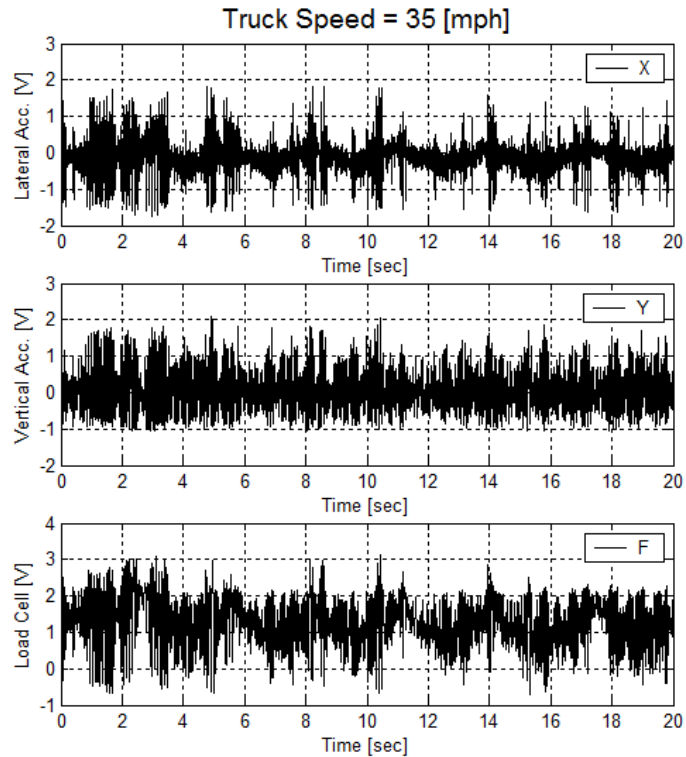


Figure 2.20 Accelerometer and Load Cell Data during Lateral Steering Maneuver

The adaptive feedforward method used to compensate for steering will be described using the experimental data in Figure 2.20, Figure 2.21 and Figure 2.22. Figure 2.20 shows raw signals from the lateral accelerometer, X, vertical accelerometer, Y and the load cell, F during an experimental test in which the driver conducted a weaving maneuver involving continuous positive and negative steering. As seen in the figure, the lateral acceleration and load cell signals contain significant high frequency noise as well as low frequency components. The low frequency component in the lateral accelerometer predominantly comes from the steering maneuver of the vehicle. The high frequency component of all three sensors comes from the vibrations in the redundant wheel. The vertical acceleration signal is not affected much by the lateral acceleration maneuvers.

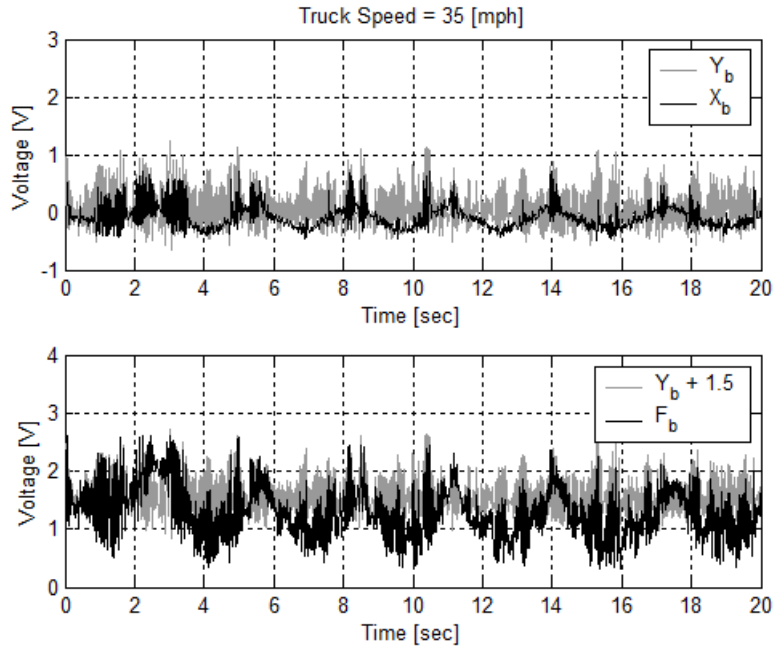


Figure 2.21 Accelerometer and Load Cell Data after Low Pass Filtering

A low pass Butterworth filter with a cut-off frequency of 10 Hz is first used to process the raw signals from the accelerometer and the load cell. The resulting filtered signals are shown in Figure 2.21. The Butterworth filtered vertical acceleration, Y_b and the lateral acceleration, X_b are shown in the upper part of the figure. The filtered load cell signal and a time-shifted offset value of the vertical acceleration, Y_b are plotted in the lower half of the figure. It can be seen that the high frequency components in the load cell signal correlate very well with the vertical acceleration signal.

Subtracting the time-shifted offset value of the filtered vertical acceleration from the filtered load cell signal produces the signal F_{Y_a} shown in the upper part of Figure 2.22. Now F_{Y_a} contains low frequency components corresponding to lateral acceleration. The lateral acceleration signal is similarly treated with Y_b being subtracted from it to produce $X_{Y_a}+0.1$. As seen in the upper part of Figure 2.22, there is high correlation between $X_{Y_a}+0.1$ and F_{Y_a} .

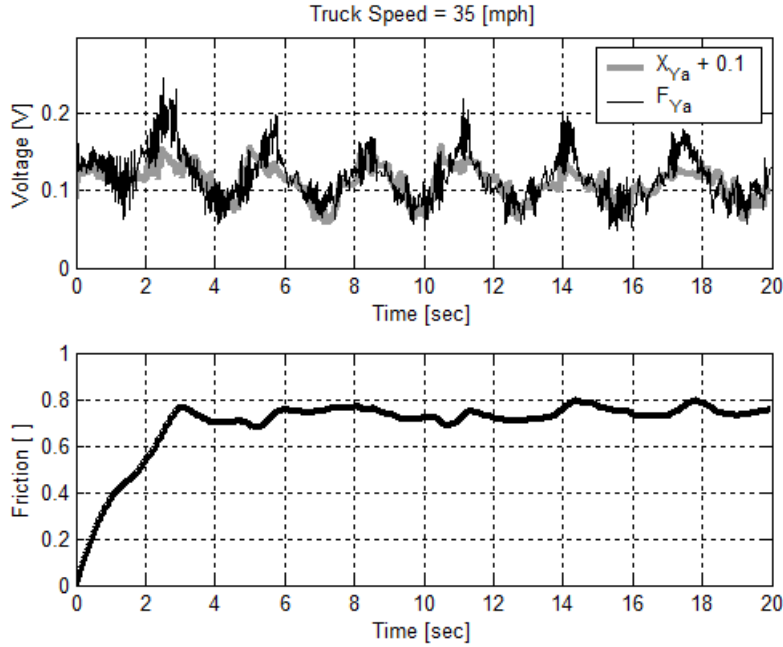


Figure 2.22 Friction Coefficient after Adaptive Estimation

An adaptive feedforward estimator is now used to filter the signal $X_{Ya}+0.1$. The difference between F_{Ya} and $X_{Ya}+0.1$ serves as the error signal to adaptively update the coefficients of the feedforward filter. The parameter h_0 serves as an estimate of the friction coefficient μ (as was the case earlier in Equation (2.15)). The lower part of Figure 2.22 shows the estimate of the friction coefficient. Starting from a value of zero, the friction coefficient estimate converges to a value around 0.8.

2.13 Biased Quadratic Mean Filter

A new filter without using an auxiliary accelerometer is also designed based on a modified quadratic mean filter (QMF) by exploiting the relationship between the mean and the variance of the force signal which is inherent in the dynamics of the proposed friction coefficient measurement system as discussed previously. The variance takes care of filtering the low frequency oscillations on the force signal, leading to a faster and better filtering performance at low frequency bands.

The definition of a QMF is given in Equation (2.18), where x_i is the sampled signal, m is the number of samples in a moving time window and N is the size of the sampled signal.

$$y_j = \sqrt{\frac{1}{m} \sum_{i=j}^{j+(m-1)} (x_i)^2} \quad j = 1 : N - (m - 1) \quad (2.18)$$

The output of QMF is nothing but the moving root mean square (RMS_j) of the signal which can be written in terms of the moving average μ_j and variance σ_j^2 of the signal as in Equation (2.19) [8].

$$y_j = RMS_j = \sqrt{\mu_j^2 + \sigma_j^2} \quad (2.19)$$

The quadratic mean filter can be modified to utilize the dynamic relationship between the mean and the variance for removing the low frequency oscillations. The biased quadratic mean filter algorithm introduces a constant bias, K which is unique to the measurement system and valid for all snowplow speeds.

$$y_j = -\sqrt{\frac{1}{m} \sum_{i=j}^{j+(m-1)} (x_i + K)^2} - K = \bar{y}_j - K \quad j = 1 : N - (m - 1) \quad (2.20)$$

The relation between the moving average μ_j and the variance σ_j^2 can be deduced from Equation (2.20), as presented in Equation (2.21).

$$y_j = -\sqrt{\sigma_j^2 + (\mu_j + K)^2} - K \quad j = 1 : N - (m - 1) \quad (2.21)$$

The proof of this relation can be given as in Equation (2.22). A Hann type weighting function is used while averaging the time windows. The Hann window is mostly effective in the filtering of high frequency bands rather than the low frequency bands.

$$\begin{aligned} \bar{y}_j &= \sqrt{\frac{1}{m} \sum_{i=j}^{j+(m-1)} (x_i + K)^2} \quad (2.22) \\ &= \sqrt{\frac{1}{m} \sum_{i=j}^{j+(m-1)} x_i^2 + \frac{1}{m} \sum_{i=j}^{j+(m-1)} 2x_i K + \frac{1}{m} \sum_{i=j}^{j+(m-1)} K^2} \\ &= \sqrt{\frac{1}{m} \sum_{i=j}^{j+(m-1)} (x_i - \mu_j + \mu_j)^2 + 2K \mu_j + K^2} \\ &= \sqrt{\frac{1}{m} \sum_{i=j}^{j+(m-1)} (x_i - \mu_j)^2 + 2\mu_j^2 - \mu_j^2 + 2K \mu_j + K^2} \\ &= \sqrt{\sigma_j^2 + (\mu_j + K)^2} \end{aligned}$$

As we have explained previously, the absolute mean value of the force signal decreases/increases whenever the variance of the force signal increases/decreases according to the physical interpretation of the system. This implies that the low frequency oscillation on the square mean value μ_j^2 signal is approximately 180° out of phase with the low frequency oscillation on the variance σ_j^2 . Hence, an appropriate bias value should be chosen so that the

oscillations on both signals cancel out each other. If the magnitude of the square mean value oscillations is less than the magnitude of variance oscillations, K should have the same sign as μ_j .

If we assume that the oscillations on the $(\mu_j + K)^2$ signal and the variance have the same magnitude and are perfectly out of phase, by adding them up we can completely remove the low frequency oscillations and find a constant output such as $y_j = A$ which only changes with respect to the friction coefficient as in .

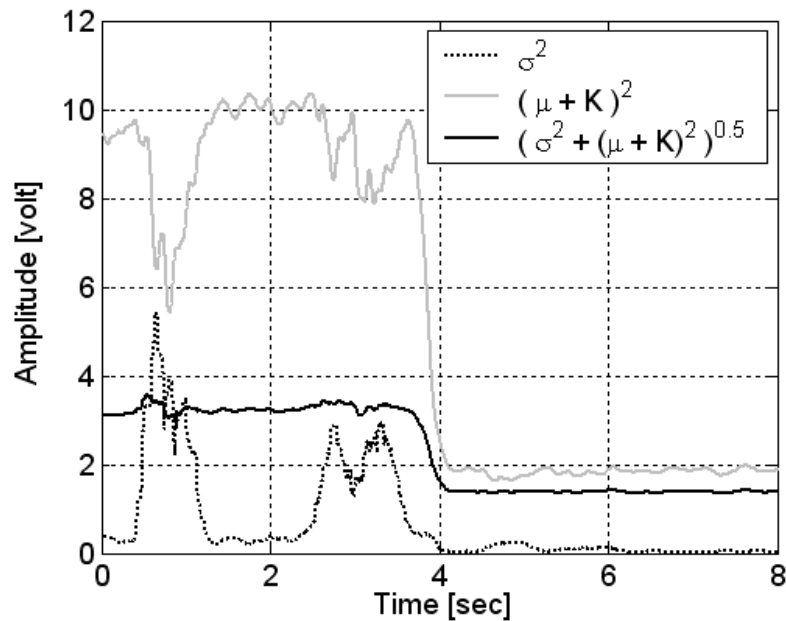


Figure 2.23 Quadratic Mean Filter Sensor Performance

The bias value relates the variance of the noise to the low frequency oscillation of the mean of the signal. A very high variance in a certain time interval means that there is no effective contact patch in that time interval. The traction between the tire and the road converges to zero, as well as the absolute mean value of the lateral tire force. If a linear relationship is assumed between variance of the noise and the reduction in the traction, a bias value can be found experimentally which is specific to the designed system. The bias depends on the mechanical parameters of the measurement system, rather than the excitation forces or the surface condition of the roadway. Refer to [9] for test results.

Chapter 3. Closed Loop Applicator Control

3.1 Friction Mapping with Automatic Vehicle Location

The performance of the designed friction wheel system together with the automated vehicle location (AVL) system is tested in a closed-to-traffic roadway located in Minnesota's Cold Weather Road Research Facility. Under cold weather conditions, a specially designed water spray system as presented in Figure 3.1 and Figure 3.2 is used. Two ice-patches are formed with an approximate length of 75 feet and with a distance of about 300 feet in between as presented in Figure 3.3. The water spray system is hooked up to a water tank located at the back of a pickup truck.

The snowplow truck starts traveling on the asphalt road from a certain distance. When the truck arrives at the first asphalt-to-ice transition region, the friction wheel immediately detects the slippery road surface. The road surface condition is measured by the force sensor and a control signal is generated to turn on the applicator based on the estimated tire-road friction coefficient. The applicator stays turned on until the truck reaches the ice-to-asphalt transition. Once the friction wheel hits the asphalt road, the friction coefficient of the roadway increases and the control signal turns off the applicator. Same steps repeat themselves for the second ice patch, as well.



Figure 3.1 Pick-Up Truck Based Water Spray System



Figure 3.2 Ice Patch Formation



Figure 3.3 Test Road

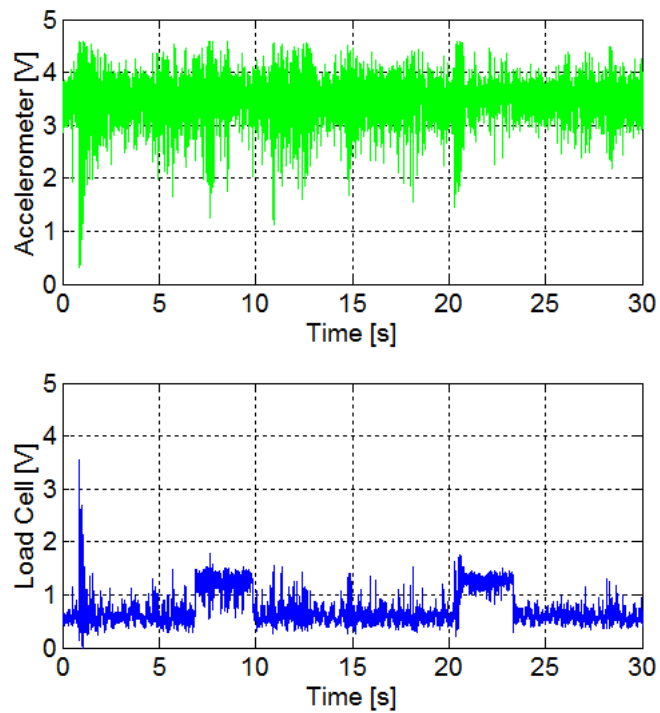


Figure 3.4 Measurement Data, Estimated Friction Coefficient

An exemplary test result for a truck traveling at about 25 mph is presented. Both the raw accelerometer and load cell signals are shown in Figure 3.4 as the truck approaches and goes over the ice patches. It is clear from the figure that it is difficult to differentiate the road surface changes from the noise on the force signal, meaning that the slippery regions cannot be detected unless the excessive noise is filtered out quickly.

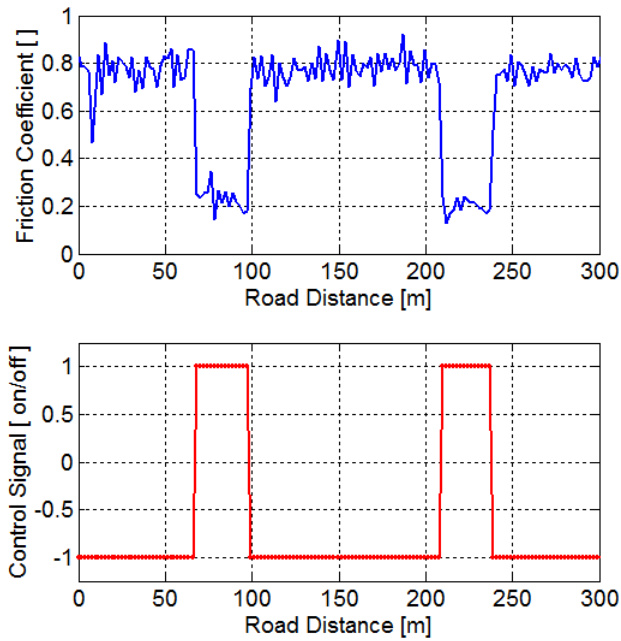


Figure 3.5 Applicator Control Signal

The estimated friction coefficient and the control signal output are presented in Figure 3.5. The developed filtering algorithm successfully removes the excessive noise on the force signal and generates a continuous control signal based on the friction coefficient estimations of two different road surface conditions. The control signal is generated using friction coefficient threshold value of 0.4 and this value has worked reliably for all of the tests executed so far while differentiating high and low friction coefficient surfaces.



Figure 3.6 Test Road in the Map

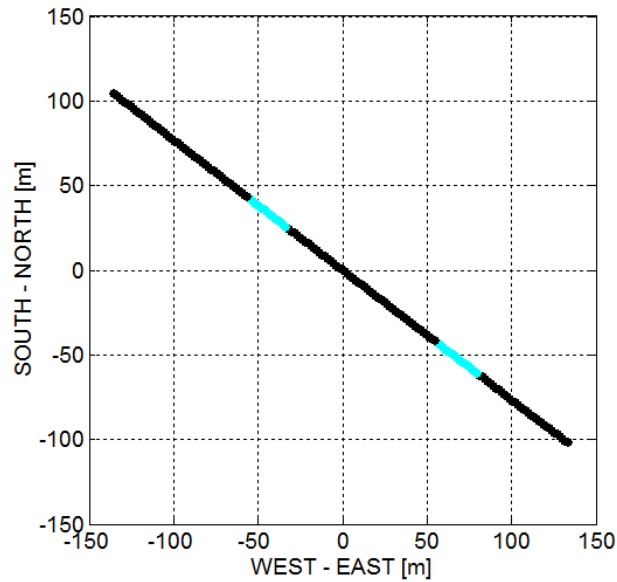


Figure 3.7 Ice Patches Locations on the Test Road

The developed friction coefficient measurement system can be coupled with the AVL system through a GPS receiver for preparing friction coefficient maps of roadways. The treated and untreated slippery spots can be marked on the map with the help of the GPS receiver which basically keeps track of the truck location. The test road in the map given in Figure 3.6 has two slippery spots on it which are marked in light blue color as shown in Figure 3.7. The GPS receiver used in the experiments is a GARMIN 18x OEM sampling at 1.0 Hz as shown in Figure 3.8.



Figure 3.8 GPS Receiver

3.2 Black Ice and Wet Surface Differentiation

Black ice is a type of slippery surface mostly seen on bridges and overpasses due to the air circulation both above and below the surface of the elevated roadway. The condensation of the automobile exhaust gas may also cause black ice on the surface of the normal roadways when the temperatures are at the lowest levels in winter time. This is a dangerous situation that threatens the roadway safety by causing serious accidents and loss of lives.

Especially in harsh winter conditions when the visibility of the roadway is decreased, distinguishing between the black ice and the wet road surface is not an easy task for a snowplow operator. Such hazardous formations on the road surface may either be overlooked by naked eye

and cause accidents or over treated in order to be on the safe side and cause increased maintenance costs. In these critical situations, the designed friction wheel system works reliably and helps the snowplow operator.



Figure 3.9 Black Ice



Figure 3.10 Wet Road Comparison

In order to test the performance of the system on black ice and wet road surfaces, the friction wheel is fixed to the rear bumper of a pickup truck and the control signal is connected to an LED that represents the applicator. The two cases when the friction wheel travels on the black ice and the wet road are presented in Figure 3.9 and Figure 3.10, respectively. In the former case, the LED sitting at the left bottom corner of the picture is turned on by the control signal due to the low friction of the black ice with respect to the dry asphalt. However, in the latter case LED is never turned on since the friction level of the wet asphalt is pretty much the same as the dry asphalt.

Measurement and friction coefficient estimation results for both cases are presented. The estimated road friction seems to drop when the friction wheel travels on the black ice as presented in Figure 3.11 (a), while staying at the same level when it travels on the wet road as given in Figure 3.11 (b). The results show that the system is able to differentiate the two surface conditions.

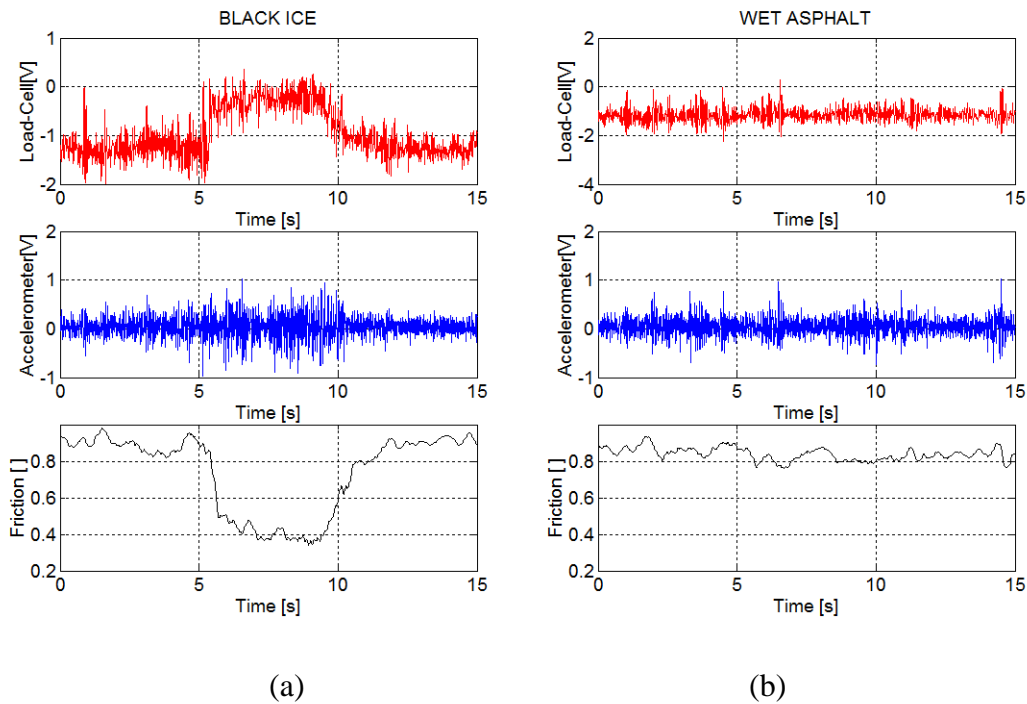


Figure 3.11 Black Ice Data and Wet Road Measurement Data

The delay of the closed-loop control system is an important parameter especially while turning on the applicator in time in order to cover the entire ice patch, i.e. before the applicator at the back of the truck reaches the asphalt-to-ice transition. A certain amount of time elapses for the processing of the measurement data and the activation of the deicing applicator after the friction wheel hits the slippery road surface. And this delay actually has two main components, namely the applicator hardware delay and the signal processing algorithm software delay. The following sections present the measurement of these two delays in order to evaluate the overall performance of the closed-loop control system.

3.3 Measurement of Snowplow Applicator Delay

After a control signal is sent to turn on the applicator, a certain amount of time elapses until the deicing material reaches to the ground. This time delay is due to the electrical and mechanical components of the applicator system and completely independent from the time elapsed for the data processing.

Applicators normally have time delays with a constant mean and certain variance. Since the length of the untreated portion of the ice patch is in distance unit, it is more intuitive to express delays in terms of the distance traveled by the truck during that time. When expressed in distance unit, applicator delays become a function of the truck speed.

Applicator delays can change dramatically depending on their mechanical design. The delays of two applicators are measured and compared to understand whether one improves the time response of the developed closed-loop control system significantly better than the other one does. The two applicators examined in this paper, namely the conventional applicator and the zero velocity applicator, are presented in Figure 3.12 and Figure 3.13, respectively.



Figure 3.12 Conventional Applicator



Figure 3.13 Zero Velocity Applicator

The conventional applicator is simply made of a spreader whose axis of rotation is normal to the ground. The target lane depends on the angular speed of the spreader. If the spreader is set to rotate at a low angular velocity, then the lane on which the truck is traveling is treated. If the spreader is set to rotate at a high angular velocity, then the adjacent lanes are treated. In our case, the spreader rotates very slowly, meaning that the deicing material particles on the spinner are also traveling at the truck speed in forward direction. Here, the angular velocity of the spinner is neglected. In other words, the particles are assumed to be in free fall with respect to an observer on the truck. This also implies that the available time for a conventional applicator is actually shorter than the available time previously obtained from the ratio between the length of the truck and the truck speed. The distance traveled by the sand particles should be subtracted from the truck length, as depicted in Figure 3.14, in order to determine the effective length of the truck. The effective length is then divided by the truck speed to obtain the actual available time.

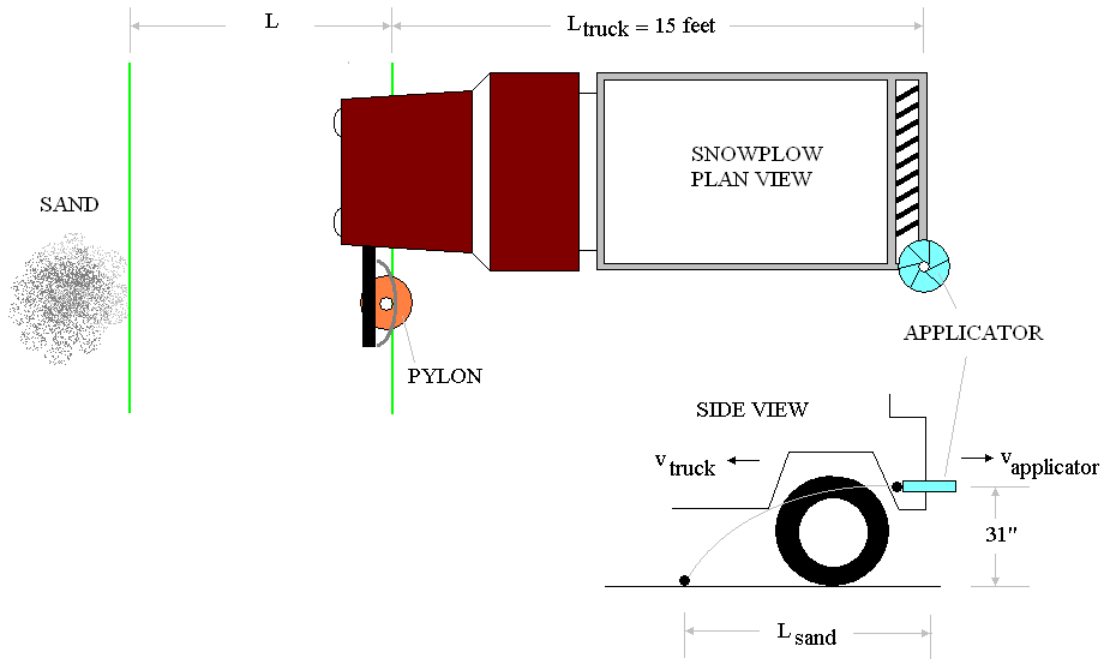


Figure 3.14 Setup for the Applicator Delay Measurement

The zero velocity applicator is another type of applicator which prevents the deicing material particles from traveling with respect to the ground. When the truck travels at a certain speed in the forward direction, the zero velocity applicator projects the deicing material at the same speed in the opposite direction with the help of a spreader whose rotation axis is parallel to the ground. Thus, the resulting speed of the particles becomes zero with respect to an observer on the roadway and this allows the operator to deploy the deicing material exactly where it is needed. Since the deicing material does not have a velocity parallel to the ground, it is now in free fall also with respect to an observer on the ground. The particles do not move relative to the ground and do not scatter away from the targeted icy spot. Thus, the zero velocity applicator is known to be more effective than the conventional applicator.

In the executed tests, the friction wheel and the filtering algorithm are excluded from the system, in order to eliminate the delays due to the friction measurement system and the software data processing. The applicator is turned on automatically by means of a special setup, when a certain point on the roadway is passed by the truck. This particular point basically substitutes the asphalt-to-ice transition, meaning that no ice-patch is used on the road surface since the friction wheel is not in use.

The setup utilized to turn on the applicator is presented in Figure 3.15. A wooden block aligned with the friction wheel is extended out from the truck to the left as shown in Figure 3.16.

The block carries a piece of wire which is hooked up to a normally closed contact. The operator drives the truck in such a way that the wooden block goes over a pylon standing on the roadway. When the loosely coupled wire is pulled off by the pylon as shown in Figure 3.16, the

broken circuit activates a relay and runs the applicator instantaneously. The time delay of this setup is negligible with respect to the measured time delays.



Figure 3.15 Location of the Wooden Block



Figure 3.16 Wire Piece/Pylon Couple

During these tests sand is used as deicing material. Since the sand particles are not easy to differentiate from the texture of the roadway, an observer outside the truck is put in charge of watching the experiment and pointing out where exactly the first sand particles fell down. If

there were no time delay, the first particles would fall down to a “no-delay” point before the pylon, and the distance between the pylon and the no-delay point would be equal to the distance between the friction wheel and the applicator. This means that the delays expressed in distance unit are supposed to be measured relative to the no-delay point which is independent from the truck speed. However, since the position of the pylon represents the surface transition and is much more meaningful than the no-delay point, the delays are measured from the first deployed sand on the roadway to the pylon. This is the same thing as shifting the origin of the reference axis a constant amount of distance in forward direction. If the forward direction is assumed to be positive, then the delays before the pylon will have negative values after shifting the origin.



Figure 3.17 Conventional Applicator Delay

The positive delay means that the first deployed sand is ahead of the pylon and some portion of the imaginary slippery surface is left untreated. The negative delay means that the first deployed sand is before the pylon and the surface coming after this point is completely treated including the imaginary slippery surface starting with the pylon.

Conventional and zero velocity applicators are compared at a truck speed of about 26 mph. At that critical speed the zero velocity applicator has no delay, whereas the conventional applicator has a delay of positive 20 feet. The measured delay of the conventional applicator is given in Figure 3.17. This proves that the zero velocity applicator performs better than the conventional applicator and it is more suitable for the developed close-loop control system.

3.4 Measurement of Friction Measurement System Delay

The delay of the developed filtering algorithm can also be measured with the same setup. In this case, an actual slippery surface is needed since the friction wheel is back in the loop. The pylon is again located at the surface transition and the on/off signal generated by the wire piece

and the pylon is hooked up to the digital input of the data acquisition card in order to record this signal and determine where exactly the low friction surface starts in time. However, this time the applicator is not controlled by the on/off signal generated by the special setup, rather by the friction wheel through the output of the algorithm.



Figure 3.18 Low Friction Plastic Surface

Since the tests are executed in spring time, a slippery plastic sheet is employed instead of an ice patch and the friction coefficient of the sheet is decreased further by spraying soap on the surface as in Figure 3.18. Although its friction coefficient is not as low as the friction coefficient of the ice patch, the plastic sheet with the soap works well for our purpose of measuring the time delay.

The measurement results are presented in Figure 3.19. The original and filtered versions of the force are given in the left upper subplot along with the threshold line in black color. The left lower subplot shows the time difference between the applicator control signal and the signal generated by the special setup. When zoomed in the right lower subplot, the time delay of the filtering algorithm is read to be about 150 milliseconds.

The time delay of the algorithm is also constant and independent from the truck speed and thus can be used to find out the distance delays at different truck speeds.

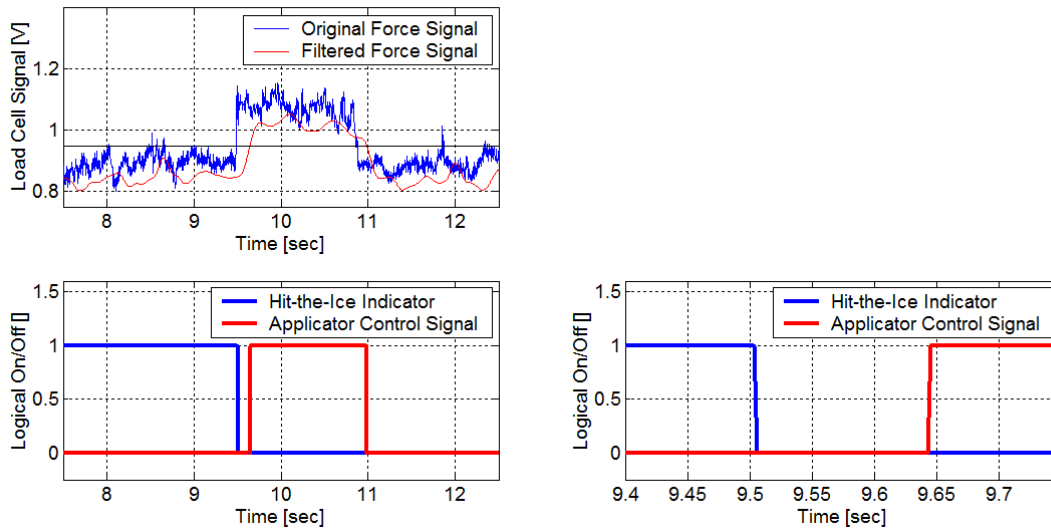


Figure 3.19 Filtering Algorithm Time Delay

3.5 Analysis of Total Delay and Closed-Loop Performance

The overall performance of the close-loop snowplow applicator is summarized in Figure 3.20. The black line at zero level indicates where the slippery surface starts, i.e. the position of the pylon. The blue color shows the distance delays of zero velocity applicator plotted against the corresponding truck speed, whereas the red color shows the total distance delays of the complete system including the filter delays. As mentioned previously, the positive delays at high truck speeds are basically the untreated length of the ice patch. The results show that the designed close-loop snowplow applicator system has zero delay at a truck speed of about 25 mph, meaning that the system can work effectively up to 25 mph. Although some portion of the ice patch is missed by the applicator beyond 25 mph, this speed is about the same as the average speed of a snowplow used in winter maintenance.

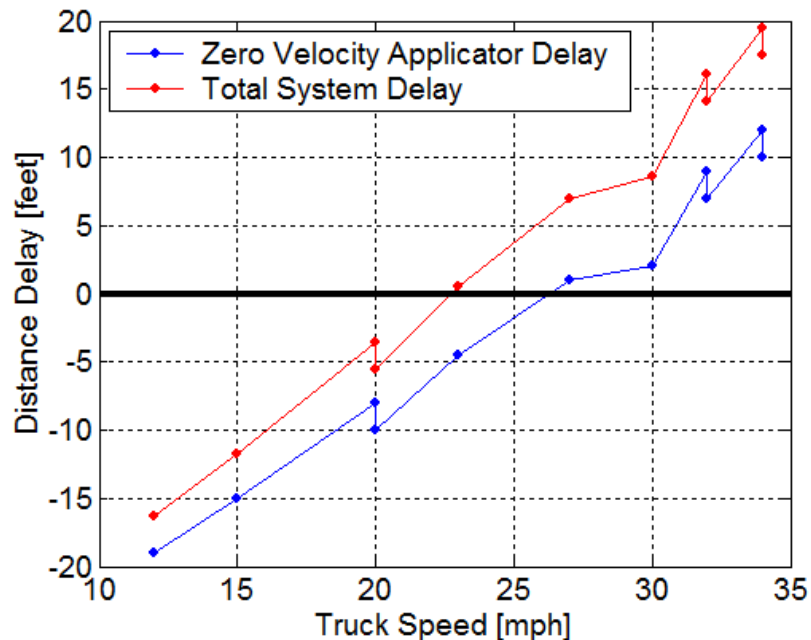


Figure 3.20 Overall System Performance

3.6 GIS Based Applicator Control

In addition to the use of tire-road friction measurement, the applicator control system is enhanced with the use of vehicle location measurements and the use of a geographical information system (GIS). The vehicle location measurement is obtained through a GPS system, the Garmin GPS 18 puck, which is the same as the GPS system utilized by the Mn/DOT MDSS system. The GPS system provides 1 Hz updates. Since the rest of the signal processing system for friction estimation requires faster sampling, a dual real-time loop is utilized. The friction estimation system runs on a 250 Hz sampling loop while the GPS updates are provided through a 1 Hz loop.

The GIS system is used to store information on road segments that require default applicator use, irrespective of the measured tire-road friction coefficient value. Road segments that need default applicator use include curves, road grades, stop signs, traffic lights and other location judged as problematic by winter road maintenance operators. With the vehicle location being measured in real-time, as the vehicle is found to be at a location where default use of the applicator is specified by the GIS, the applicator is automatically controlled to apply salt/chemical to the road at that location.

The software developed for the GIS system resides on the microprocessor and is written in the C language. The user interface for the applicator control system is shown in Figures 3.21 – 3.23. At the first screen (shown in Figure 3.21), the snowplow operator can decide whether to turn on automatic applicator control, quit automatic operation or create a new map for the GIS system (for a new route). The creation of a new map has the user interface shown in Figure 3.22.

The operator can record GPS locations for the route and manually indicate road segments which need extra applicator use by clicking on appropriate buttons (such as “Stop Sign,” “Bridge,” “Intersection,” etc.). In addition the software automatically calculates road curvature and road grade angle by use of recorded GPS measurements. These measurements are used to automatically designate curved road sections as segments where default applicator use is required.

An example of a road map and its display is shown in Figure 3.24. This display will be on the screen when the snowplow is under automatic applicator control. The large red button indicates that the applicator is currently in use (due to either low friction coefficient or other default scenario). The yellow segments on the map indicate those road segments where default applicator use will be made.



Figure 3.21 First User Interface Screen



Figure 3.22 User Interface for Map Creation Software

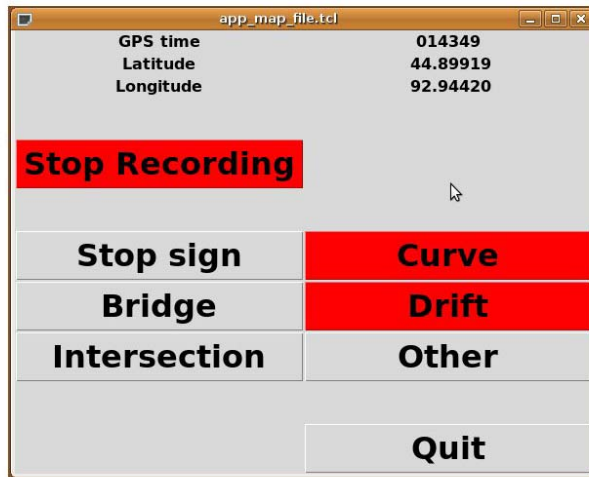


Figure 3.23 Use of Map Creation Software

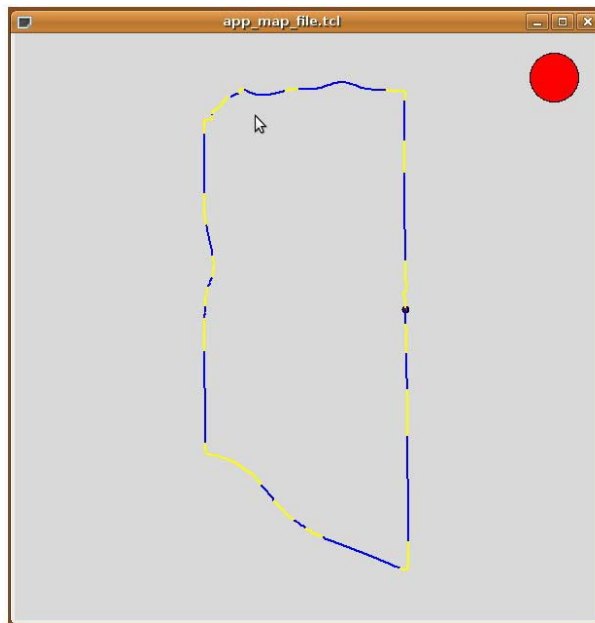


Figure 3.24 Road Map Displayed During Automatic Applicator Control

3.7 Description of Hardware

The major hardware components of the closed-loop applicator control system include

- a) The friction measurement wheel
- b) A microprocessor
- c) A LCD touch panel
- d) A GPS puck
- e) Electronic interface between the microprocessor and the Dickey John controller for the applicator on the snowplow

The above components are shown in Figures 3.25 – 3.29.

The friction measurement wheel is modular and consists of two parts: a lower instrumented wheel and an upper mounting assembly. The lower instrumented wheel consists of a tire, accelerometers and force load cell as described earlier in Chapter 2. The lower instrumented wheel is common to all vehicle configurations. The upper mounting assembly is tailored to suit the specific wheel on which the friction measurement system needs to be mounted. Two types of vehicles have been instrumented with the friction measurement system in this project – a snowplow and a pick-up truck. Photographs of the friction measurement system on the snowplow were provided earlier in Chapter 2. A photograph of the friction measurement system on a pick-up truck can be seen in Figure 3.25.

The microprocessor and its enclosure dimensions are shown in Figure 3.27 and Figure 3.26 respectively. The microprocessor includes an ARM 9 chip as its central processor and can operate on 12 V power directly from the battery of the vehicle. An inverter is not required, since AC power supply is not needed. The microprocessor is able to read analog sensor signal with an analog-to-digital converter and is also able to read serial port RS 232 signals, as shown in Figure 3.29. The load cell and accelerometers are interfaced through the analog-to-digital signal ports on the microprocessor. The GPS unit is interfaced through the RS 232 port. The cost of the microprocessor, including the data acquisition electronics is approximately \$450. The cost of the 7-inch LCD display, shown in Figure 3.28, is approximately \$300.



Figure 3.25 Friction Measurement System Installed on Pick-Up Truck

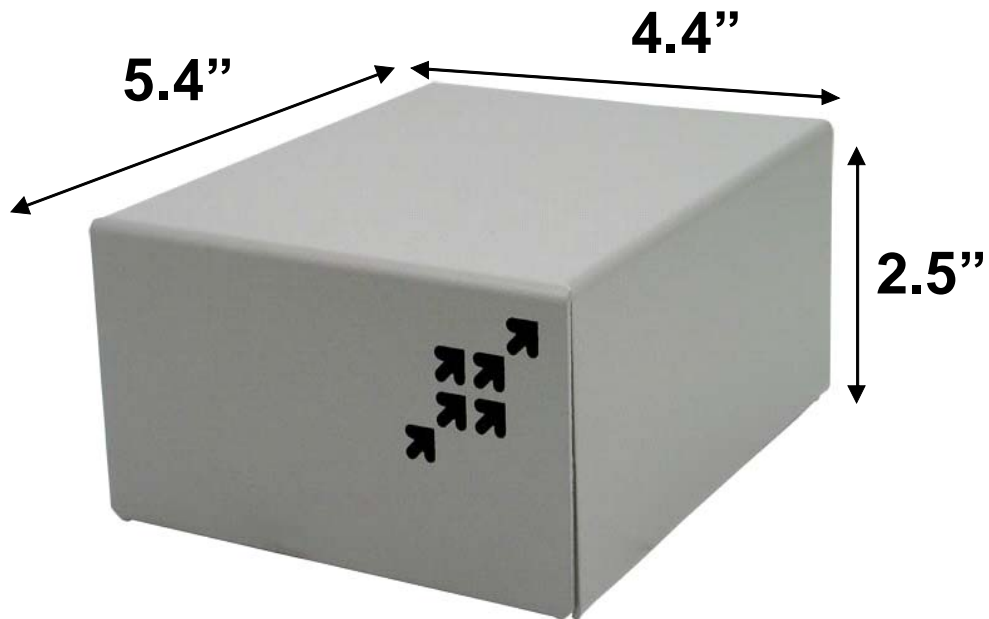


Figure 3.26 Microprocessor Enclosure Dimensions

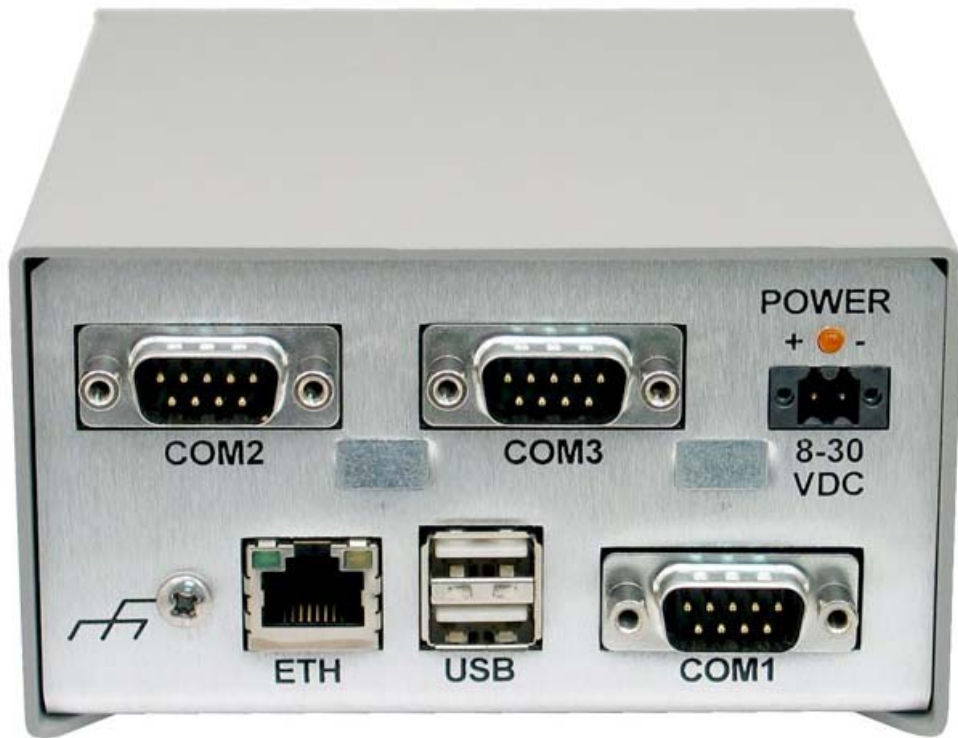


Figure 3.27 Interface Ports on Microprocessor

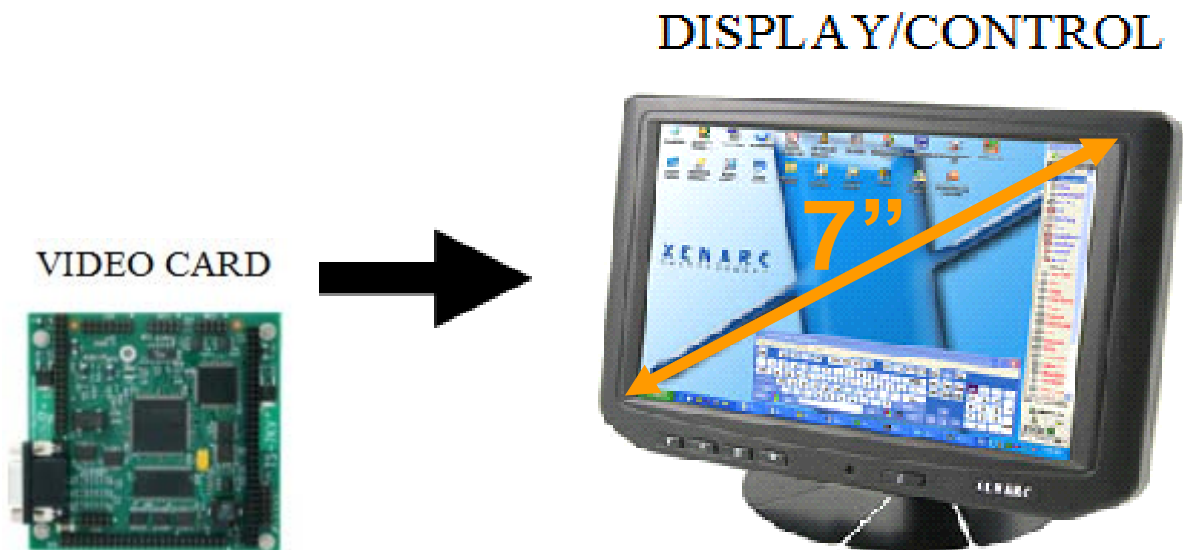


Figure 3.28 Video Card and LCD Display

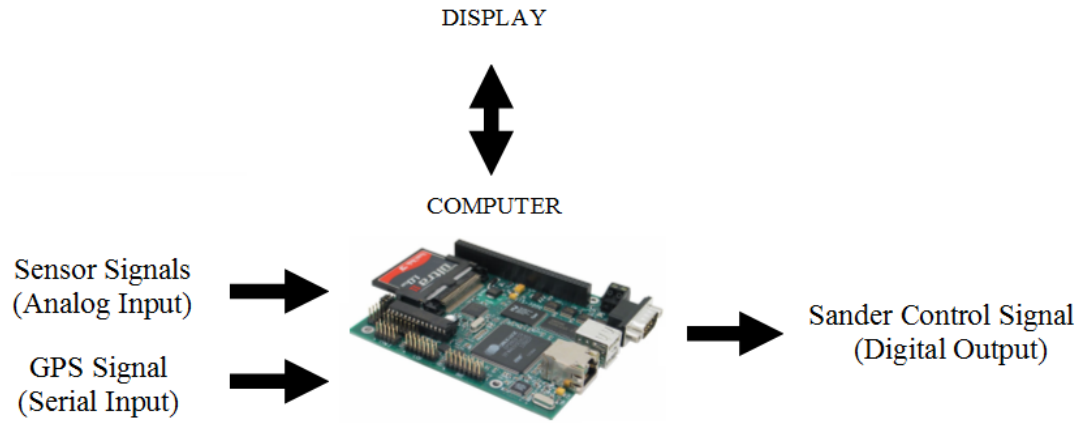


Figure 3.29 Microprocessor and Its Input-Output Interfaces

Chapter 4. Conclusions

This project conducted a detailed evaluation of a new wheel-based tire-road friction measurement system and an associated closed-loop applicator control system for a snowplow. The developed small wheel based friction measurement system provides a continuous measure of the tire-road friction coefficient and records the friction coefficient as a function of GPS-measured vehicle location. The recorded friction coefficient data provides a map of the road condition values over the entire snowplow route. This data can not only serve as a performance measure for how well roads are being maintained in winter, but can also be provided to commuters for their trip planning. Most important, the measured friction coefficient is used in this project as a real-time feedback signal to control the applicator on a snowplow.

The applicator on the snowplow is controlled to automatically turn on when the measured friction coefficient is below a set threshold. The friction measurement system is located near the front axle of the snowplow while the applicator is located at the back of the snowplow. Hence any slippery road surface must be detected from a measure of its friction coefficient quickly so that the applicator can be turned on before it reaches the slippery surface location measured by the friction measurement system. This project addressed several significant issues related to vibrations and vehicle maneuvers to quickly detect changes in friction coefficient of the road surface. In particular, algorithms were developed based on adaptive cancellation techniques, which utilized accelerometer data to remove the influence of vibrations and vehicle maneuvers.

Experimental measurements show that the friction measurement system works reliably and can detect friction coefficient changes in less than 150 milliseconds (ms). Hence a signal to turn on the applicator can be sent to the applicator in less than 150 ms after a slippery road is detected. However, the applicator on a snowplow itself has an associated hardware delay. An applicator can take several hundred milliseconds to deploy salt/chemical after it receives a turn-on signal. Furthermore, the salt/chemical from a typical applicator tends to move in the direction of snowplow travel after deployment by the applicator due to its inertia. This can cause the salt to miss the detected slippery spot. A zero-velocity applicator overcomes this problem and deploys salt/sand with zero absolute velocity so that it has minimal movement in the snowplow travel direction after deployment.

Measurements made in the project show that a zero velocity applicator controlled by a friction measurement system can reliably deploy salt/chemical on all detected slippery spots for snowplow speeds up to 25 mph. Since a snowplow speed of 25 mph is adequate for many winter maintenance operations, the developed closed-loop applicator control system is likely to be valuable as a winter road maintenance tool.

The closed-loop applicator control system was also enhanced with a GPS based geographical information system for automatic deployment of the applicator at problematic road locations. Software was developed to create road maps in which problematic road locations are pre-identified for default applicator use. The software automatically calculates road curvatures and road grade angles. It also allows the map-creator/snowplow operator to mark particular road

segments for default applicator use. Such road segments could include wind drift areas, stop signs, traffic lights, bridges and other locations deemed problematic by the operator.

The developed closed-loop system is modular, compact, inexpensive and works reliably both in recording friction coefficient as function of vehicle location and also in automatic applicator control.

Future work in this technology should focus on a limited deployment of the developed technology on a few snowplows and supervisor pick-up trucks. This would allow field evaluation of the developed technology by snowplow operators and also by supervisors for planning of winter maintenance operations.

References

- [1] L. Baker, "The Trouble with Road Salt," Star Tribune, March 22, 2008, Can be read online at <http://www.startribune.com/opinion/commentary/16912511.html>. Accessed December 8, 2009.
- [2] P. Agrawal, "Alternate Approach for the Estimation of Slip Angle and Tire-Road Friction Coefficient Using Piezoelectric Sensors", M.S. Thesis, Department of Mechanical Engineering, University of Minnesota, February, 2005.
- [3] "Highway Statistics Publications, Highway Finance Tables SF-4C and LGF-2," 1997 to 2005, <http://www.fhwa.dot.gov/policy/ohpi/hss/hsspubs.cfm>. Accessed December 8, 2009.
- [4] L. Al-Qadi, A. Loulizi, G.W. Flintsch, D.S. Roosevelt, R. Decker, J.C. Wambold, W.A. Nixon, *Feasibility of Using Friction Indicators to Improve Winter Maintenance Operations and Mobility*, Transportation Research Board (TRB)'s National Cooperative Highway Research Program (NCHRP) Web Document 53, November, 2002, <http://www.trb.org/news>. Accessed December 8, 2009.
- [5] K. Balke, P. Songchitruksa, H. Liu, R. Brydia, D. Jasek, and R. Benz, *Concepts for Managing Freeway Operations During Weather Events*, Texas Transportation Institute, Technical Report, Report No: FHWA/TX-07/0-5278-1, February, 2007.
- [6] J. Wang, P. Agrawal, L. Alexander, R. Rajamani, "An Experimental Study with Alternate Measurement Systems for Estimation of Tire-Road Friction Coefficient", *Proceedings of the 2003 American Control Conference*, Denver, CO, June, 2003.
- [7] US Department of Transportation, Federal Highway Administration, Road Weather Management Program Website: <http://ops.fhwa.dot.gov/weather>. Accessed December 8, 2009.
- [8] R. Johnson, I. Miller, J.E. Freund, *Miller and Freund's Probability and Statistics for Engineers*, Upper Saddle River, NJ: Pearson Prentice Hall, August, 2004.
- [9] G. Erdogan, L. Alexander, R. Rajamani, "Friction Coefficient Measurement for Autonomous Winter Road Maintenance", *Vehicle System Dynamics*, Volume 47, No. 4, April, 2009, pp. 497 – 512.